

---

Mechanical Engineering Theses

Mechanical Engineering

---

11-8-2019

## Physicochemical Properties of Blend Poly (Vinyl Alcohol) and Sodium Alginate Membranes for Potential Application in Wound Dressings

Martha Pieper

Follow this and additional works at: [https://scholarworks.uttyler.edu/me\\_grad](https://scholarworks.uttyler.edu/me_grad)

 Part of the Higher Education Commons, Mechanical Engineering Commons, and the Medicinal and Pharmaceutical Chemistry Commons

---

### Recommended Citation

Pieper, Martha, "Physicochemical Properties of Blend Poly (Vinyl Alcohol) and Sodium Alginate Membranes for Potential Application in Wound Dressings" (2019). *Mechanical Engineering Theses*. Paper 9.

<http://hdl.handle.net/10950/2315>

This Thesis is brought to you for free and open access by the Mechanical Engineering at Scholar Works at UT Tyler. It has been accepted for inclusion in Mechanical Engineering Theses by an authorized administrator of Scholar Works at UT Tyler. For more information, please contact [tgullings@uttyler.edu](mailto:tgullings@uttyler.edu).

PHYSICOCHEMICAL PROPERTIES OF BLEND POLY(VINYL ALCOHOL) AND  
SODIUM ALGINATE MEMBRANES FOR POTENTIAL APPLICATIONS IN  
WOUND DRESSINGS

by

MARTHA PIEPER

A thesis submitted in partial fulfillment  
of the requirements for the degree of  
Master of Science  
Department of Mechanical Engineering

Shih-Feng Chou, Ph.D., Committee Chair

College of Engineering

The University of Texas at Tyler  
December 2019

The University of Texas at Tyler  
Tyler, Texas

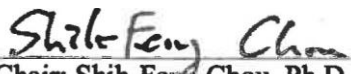
This is to certify that the Master's Thesis of

MARTHA PIEPER

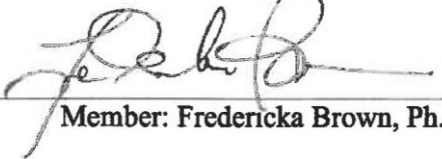
has been approved for the thesis requirement on  
November 8, 2019

for the Master of Science  
degree

Approvals:

  
Thesis Chair: Shih-Feng Chou, Ph.D.

  
Member: Chung Hyun Goh, Ph.D.

  
Member: Fredericka Brown, Ph.D.

  
Chair, Department of Mechanical Engineering

  
For JK

Dean, College of Engineering

The style and format of this thesis are in accordance with **Materials Science and Engineering C: Materials for Biological Applications**. The following referred journal papers and conference proceedings were products of the M.S. degree:

**Referred Journal Articles:**

- [1] M. Small, A. Faglie, A. Craig, **M. Pieper**, V. Fernand Narcisse, P. Neuenschwander, S.F. Chou, Nanostructure-enabled and macromolecule-grafted surfaces for biomedical applications, *Micromachines* 9 (2018) 243. doi:10.3390/mi9050243.
- [2] M. Gizaw, A. Faglie, **M. Pieper**, S. Poudel, S.F. Chou, The role of electrospun fiber scaffolds in stem cell therapy for skin tissue regeneration, *Med One* 4 (2019) e190002.

**Conference Proceedings:**

- [1] **M. Pieper**, S.F. Chou, Set theory and proofs, In Proceedings of the 2018 ASEE Gulf-Southwest Section Annual Meeting, (2018), Austin TX.
- [2] **M. Pieper**, S.F. Chou, Crosslinking of polymeric films for enhanced mechanical properties in wound dressing, submitted the 2019 ASEE Gulf-Southwest Section Annual Meeting.

## Acknowledgements

This thesis is a result of many months of research and hard work. First of all, I would like to thank Dr. Shih-Feng Chou (Department of Mechanical Engineering, College of Engineering, The University of Texas at Tyler) for his collaboration and support. It has truly been a privilege to have the opportunity to complete my Master of Science thesis under his guidance. My special thanks go to committee members, Dr. Chung Hyun Goh and Dr. Fredericka Brown for the valuable advices on the thesis work. I would also like to thank Mr. Mulugeta Gizaw, a senior lab member, for helping me understand laboratory procedures at the beginning of my research project and for his continuous intellectual inputs. I wish to thank my classmates, Addison Faglie, Alex Craig, and others for their support and encouragement. Lastly, I would like to thank my family for believing in me all the while.

## Table of Contents

List of Tables .....	iii
List of Figures .....	iv
Abstract .....	viii
Chapter 1: Introduction .....	1
Chapter 2: Significance.....	6
Chapter 3: Literature Review .....	8
3.1 Wound healing stages .....	8
3.2 Topical dressings for wound healing .....	13
3.2.1 Biocompatibility .....	15
3.2.2 Gels .....	16
3.2.3 Films .....	18
3.3 Sodium alginate in wound healing.....	21
3.4 Polyvinyl alcohol (PVA) in wound healing.....	24
3.5 Crosslinking mechanism .....	27
Chapter 4: Materials and Methods .....	31
4.1 Materials .....	31
4.2 Preparation of polymer solutions .....	31
4.3 Fabrication of films.....	32
4.4 Preparation of crosslinking solutions.....	33
4.5 Crosslinking procedures .....	34
4.6 Physical properties characterizations .....	35
4.7 Fourier-transform infrared spectroscopy .....	36
4.8 Mechanical Testing .....	36
Chapter 5: Results and Discussion.....	38
5.1 Physical properties PVA films .....	38
5.2 Physical properties of SA films .....	40
5.3 Physical properties of blend PVA/SA films.....	42
5.4 Chemical analyses: FTIR.....	46
5.5 PVA-SA Mechanical Properties.....	48
5.7 Physical properties of blend PVA/SA films.....	52
5.8 Chemical analyses: FTIR.....	56

5.9 PVA-SA Mechanical Properties.....	60
Chapter 6: Conclusions and Future Work.....	64
References.....	67

## List of Tables

<b>Table 1.</b> Applications of topical gels in wound healing. ....	17
<b>Table 2.</b> The uses of film-based dressings in wound healing.....	19
<b>Table 3.</b> Alginate film-based dressings in wound healing. ....	23
<b>Table 4.</b> Topical film-based dressings from blend polyvinyl alcohol (PVA) and natural polymers.....	26
<b>Table 5.</b> Characteristics peaks observed on crosslinked PVA/SA films with CaCl <sub>2</sub> and boric acid for 5, 10, and 30 minutes and a PVA/SA blank film. ....	48
<b>Table 6.</b> Mechanical properties of PVA/SA films crosslinked in CaCl <sub>2</sub> , boric acid, and mixture of CaCl <sub>2</sub> /boric acid solutions for 5, 10, and 30 minutes.....	51
<b>Table 7.</b> Characteristics peaks observed on crosslinked PVA/SA films with CaCl <sub>2</sub> and boric acid for 5, 10, and 30 minutes and a PVA/SA blank film. ....	59
<b>Table 8.</b> Mechanical properties of PVA/SA films crosslinked in the mixture of CaCl <sub>2</sub> /boric acid solution for 5, 10, and 30 min. ....	63

## List of Figures

<b>Figure 1.</b> Hospital discharge rates for ulcer per 1,000 diabetic population by age from 1988 to 2007. Data re-plotted according to the Diabetes Public Health Resource obtained from Centers for Disease Control and Prevention [4].	2
<b>Figure 2.</b> Classifications of wound dressing [6].	3
<b>Figure 3.</b> The interactions between platelets, blood, lymph, and fibrin cause the formation of blood clots during the hemostasis and coagulation stage [18].	9
<b>Figure 4.</b> During the inflammation stage, leukocytes and monocytes migrate into the wound, where chemoattractants for neutrophils are released from damage tissue as the mediators [18].	11
<b>Figure 5.</b> During the proliferation phase, endothelial cells sprout and granulate, whereas fibroblasts and collagen contribute to the formation of a mature extracellular matrix (ECM) [18].	12
<b>Figure 6.</b> Remodeling and maturation of the extracellular matrix (ECM) foment the diminishing of collagen, cellular, and vascular contents within the ECM and promoting the thickening of epidermis as the epithelium stratifies [18].	13
<b>Figure 7.</b> Molecular structure of alginic acid containing $\beta$ -D-mannuronic acid (m), and $\alpha$ -L-guluronic acid (n) residues.	22
<b>Figure 8.</b> Structure of alginate and its binding of calcium cations in egg-box model [63].	22
<b>Figure 9.</b> Molecular structure of polyvinyl alcohol with repeating monomer of $\text{CH}_2\text{CHOH}$ .	25

**Figure 10.** Representation of the molecular structure in PVA films during the aqueous boric acid crosslinking at different concentrations [84].....29

**Figure 11.** Representation of the egg-box model in low and high CaCl<sub>2</sub> concentration. The red solid circles depict calcium cations located between guluronic acid residues [90]......30

**Figure 12.** Polymeric solution making process showing (A) raw polymer powder (image represents PVA powder), (B) PVA powder in deionized water before the mixing process, and (C) solution stirring and heating process using a stirring hot plate.....32

**Figure 13.** Solvent casting method for fabrication of the polymer films of (A) PVA film, (B) SA film, and (C) blend PVA/SA film.....33

**Figure 14.** Various crosslinking solutions for pure PVA, pure SA, and blend PVA/SA films showing (A) CaCl<sub>2</sub> solution, (B) boric acid solution, and (C) mixture of CaCl<sub>2</sub>/boric acid solution. ....34

**Figure 15.** (A) Schematic of a rectangular specimen used in tensile testing (unit = mm). (B) Crosslinked set of five sample films ready for the mechanical test. Both ends of the rectangular sample films were attached to labeling tapes to enhance gripping on the mechanical tester. (C) Typical stress strain curve for a PVA/SA sample film. The representative curve was depicted from a sample crosslinked with CaCl<sub>2</sub> for 5 minutes. ....37

**Figure 16.** PVA sample films crosslinked for 5, 10, and 30 minutes with CaCl<sub>2</sub>, boric acid, and mixture of CaCl<sub>2</sub>/boric acid solutions. Photos depict from sample discs before and after crosslinking. Scale bars = 10 mm. ....38

**Figure 17.** Percent weight change of PVA sample films crosslinked with CaCl<sub>2</sub>, boric acid, and mixture of CaCl<sub>2</sub>/boric acid solutions for 5, 10, and 30 minutes. ....40

**Figure 18.** SA sample films crosslinked for 5, 10, and 30 minutes in CaCl<sub>2</sub>, boric acid, and mixture of CaCl<sub>2</sub>/boric acid solutions. Photos depict from sample films before and after crosslinking. SA dissolved in boric acid, and therefore, no images for the comparison. Scale bars = 10 mm. ....41

**Figure 19.** Percent weight change of SA sample films crosslinked with CaCl<sub>2</sub> and mixture of CaCl<sub>2</sub>/boric acid solutions for 5, 10, and 30 minutes. SA sample films crosslinked with boric acid were dissolved, and therefore, data were excluded. ....42

**Figure 20.** PVA/SA sample films crosslinked for 5, 10, and 30 minutes in CaCl<sub>2</sub>, boric acid, and mixture of CaCl<sub>2</sub>/boric acid solutions. Photos depict from sample films before and after crosslinking. ....43

**Figure 21.** PVA/SA sample films crosslinked with CaCl<sub>2</sub>, boric acid, and mixture of CaCl<sub>2</sub>/boric acid solutions for 5, 10, and 30 minutes, showing (A) percentage weight change, (B) percentage area change, and (C) percentage thickness change. ....45

**Figure 22.** FTIR spectra of uncrosslinked PVA/SA sample films (blank) and crosslinked PVA/SA sample films with (A) boric acid, (B) CaCl<sub>2</sub>, (C) and CaCl<sub>2</sub>/boric acid solutions for 5, 10, and 30 minutes. ....47

**Figure 23.** Mechanical properties of PVA/SA films, showing (A) average elastic modulus and (B) average tensile strength after crosslinking in CaCl<sub>2</sub>, boric acid, and the mixture of CaCl<sub>2</sub>/boric acid solutions for 5, 10, and 30 minutes. ....50

<b>Figure 24.</b> PVA/SA sample films crosslinked for 5, 10, and 30 minutes in mixture of CaCl <sub>2</sub> /boric acid solutions. Photos show from sample films before and after crosslinking. ....	53
<b>Figure 25.</b> PVA/SA sample films crosslinked with the mixture of CaCl <sub>2</sub> /boric acid solutions for 5, 10, and 30 minutes. ....	55
<b>Figure 26.</b> FTIR spectra of uncrosslinked blank PVA/SA films (Control) and crosslinked PVA/SA films with a mixture of CaCl <sub>2</sub> /boric acid solutions for 5, 10, and 30 minutes, showing (a) 5wt%/1wt% PVA/SA, (b) 6wt%/1.2wt% PVA/SA, and (c) 7wt%/1.4wt% PVA/SA. ....	58
<b>Figure 27.</b> Mechanical properties of PVA/SA films showing (a) average elastic modulus and (b) average tensile strength after crosslinking in the mixture of CaCl <sub>2</sub> /boric acid solutions for 5, 10, and 30 minutes. ....	62

## Abstract

### PHYSICOCHEMICAL PROPERTIES OF BLEND POLY(VINYL ALCOHOL) AND SODIUM ALGINATE MEMBRANES FOR POTENTIAL APPLICATIONS IN WOUND DRESSINGS

Martha Pieper

Thesis Chair: Shih-Feng Chou, Ph.D.

The University of Texas at Tyler  
December 2019

Poly(vinyl alcohol) (PVA) and sodium alginate (SA) are water-soluble polymers with excellent biocompatibility suitable for biomedical applications in wound dressings. In this study, pure PVA, pure SA, and blends of PVA/SA membranes were solvent cast into films followed by crosslinking in  $\text{CaCl}_2$ , boric acid, and a mixture of  $\text{CaCl}_2$ /boric acid solutions for 5, 10, and 30 minutes. Initial feasibility studies showed a strong correlation of film thickness to the observed mechanical properties. Further studies in solvent casting of blend PVA/SA films, using various polymer concentrations, yielded better film appearance with minimal physical changes after crosslinking. The corresponding chemical structures of the PVA/SA films after crosslinking suggested a consolidated molecular packing network, resulting in the increases of their mechanical properties. In general, this work demonstrates the feasibility of solvent casting as well as crosslinking of the polymer films with the intention to provide information in design and manufacturing of wound dressing materials.

## Chapter 1: Introduction

According to the World Health Organization, approximately 325 millions of people globally will be affected by diabetes by the year 2025 [1]. Among these people, around 15% of them will experience a foot ulcer in their lifetime, where amputation is the inevitable outcome if these foot ulcers are not treated properly [2]. These chronic foot ulcers are hard to heal and are more pronounced in aging populations than young adults [3]. In addition, data reported by the Centers for Disease Control and Prevention, shown in Figure 1, demonstrates that elderly people continuously receive the highest ulcer development rate, per 1000 diabetic patients, than other age groups from 1988 to 2007 [4]. In the U.S., these chronic wounds affect 6.5 millions of people with a total amount of approximately \$25 billion dollars spent annually on wound related treatment procedures [3]. In another study, based on the data from the center for disease control (CDC), in 2010, 8.3% of the US population (308,745,538) roughly 25, 625,880 Americans were affected by diabetes. In particular, Medicare spent about \$ 1.5 billion per year on the diabetic foot ulcer treatment, that is a cost per ulcer ranging around \$3,000 to \$108,000 [5]. These statistics suggest the need for the development of a better treatment strategy to enhance wound healing, ideally, through the design and manufacturing of a dressing material with therapeutic effectiveness and efficacy.

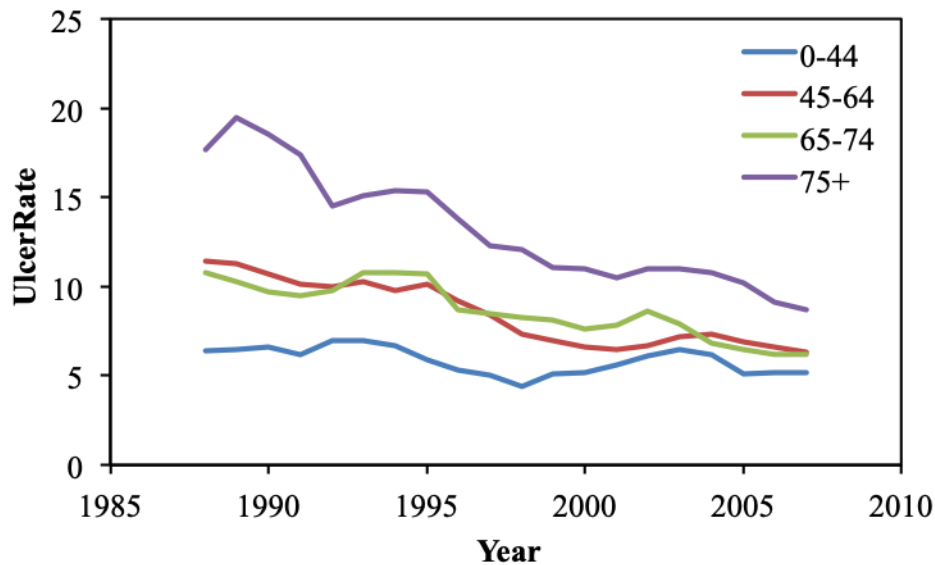


**Figure 1.** Hospital discharge rates for ulcer per 1,000 diabetic population by age from 1988 to 2007. Data re-plotted according to the Diabetes Public Health Resource obtained from Centers for Disease Control and Prevention [4].

A wound depicts an injury on the skin caused by thermal or physical mean or as a side effect of a physical condition. In diabetic foot ulcers, the healing process is prolonged that it becomes a chronic health issue, where the high blood glucose at the wound site tends to make it prone to bacterial infections by *Escherichia coli* (*E. coli*), *Bacillus subtilis* (*B. subtilis*), etc. Maintaining a healthy wound condition that prevents the local tissues from bacterial infections alleviates the immune responses, which facilitates healing. Therefore, the engineering design criteria in development of topical wound dressings include the requirements that these materials should be: (1) impermeable to outer environment and bacteria, (2) allowing gas/nutrient exchanges, and (3) providing thermal isolation to the wound site.

Owing to the advancement in polymer technology, various topical formulations of wound dressings have emerged on the market in the forms of films, porous scaffolds, hydrogels, nanoparticles, and fibers, as shown in Figure 2 [6]. The sophisticated gamut of dressings is the consequence of diversity in types of wounds, resulting in product specific aims to resolve various types of wounds [7]. It is well known that controlling the moisture balance in the wound bed accelerates the healing process. Hence, in the design aspect, one of the functions in topical dressings is to be able to absorb wound exudate while allowing a moist environment in the wound area [8].

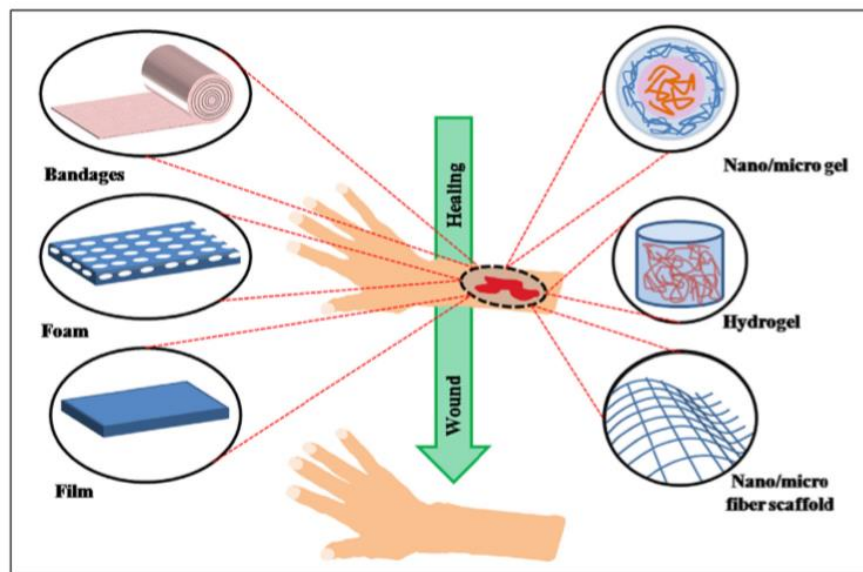


**Figure 2.** Classifications of wound dressing [6].

The current available wound dressing materials on the market are mainly fabricated from pure synthetic polymers, pure natural polymers, or blends of these two [9]. Some natural polymers that benefit wound healing include chitosan obtained from crab shells, agar extracted from seaweeds, sericin (a gumming protein) acquired from silk

fibers [9], keratin derived from chicken feathers [10], and sodium alginate (SA) obtained from brown algae. For synthetic polymers, the most common materials used in wound dressings are poly (lactic acid) (PLA), poly(lactic-co-glycolic) acid (PLGA), polycaprolactone (PCL), polyvinyl alcohol (PVA), and polyurethane (PU) [11]. Among them, PVA, SA, and their physical blends (PVA/SA) are being considered for the used in manufacturing of wound dressings due to its flexibility, adhesively, and transparency characteristics, allowing the visualization of the wound without disturbance to the injure area.

Due to the increasing popularity in using solid dosages from polymers for design and manufacturing of wound dressings, the structure-property relationships of blend polymers as drug carriers are of particular interest. Therefore, the objective of this thesis work is to synthesize membranes from blends of PVA/SA solutions followed by characterizations of the physicochemical properties of the membranes, and then use the insight gained, to inform future applications in drug carriers for wound healing.

To achieve the objective of this thesis work, films from pure PVA (5 wt%), pure SA (1 wt%), and the 50/50 blend of PVA/SA were made to explore their corresponding physicochemical properties. In order to adjust their properties, post treatments of the films involved in crosslinking in solutions of  $\text{CaCl}_2$ , boric acid, and the 50/50 blend of  $\text{CaCl}_2$ /boric acid for 5, 10, and 30 minutes. Physicochemical characterizations and mechanical testing showed a strong correlation of the film properties on their thickness. This finding led to the investigation of film preparation process that optimized the thickness of the films. In general, the results from this thesis work suggest that the blend

PVA/SA films crosslinked with  $\text{CaCl}_2$ /boric acid solution enhanced the chemical and mechanical properties of the hybrid film, which are essential qualities for polymers intended for use in the medical field as a wound dressing or drug-releasing membrane.

## Chapter 2: Significance

The uniqueness of this thesis work is to fabricate blend polymer membranes from water-soluble polyvinyl alcohol (PVA) and sodium alginate (SA) followed by crosslinking them in water-based crosslinking agents of boric acid and  $\text{CaCl}_2$ . Crosslinking of SA is typically done in  $\text{CaCl}_2$  solutions by utilizing divalent cations of  $\text{Ca}^{2+}$  to form a compact three-dimensional molecular network through the linking of the free carboxyl and hydroxyl groups. In order to simultaneously crosslink the blend PVA/SA membranes, a liquid-based boric acid solution was used to crosslink PVA in the blend membranes. However, this approach yields a potential problem in polymer dissolution during crosslinking due to the high solubility of PVA and SA in water. Our results showed that the blend PVA/SA membranes exhibited minimal changes in physical properties, suggesting a negligible dissolution effect in the PVA/SA membranes after crosslinking. Chemical analysis displayed the formation of the intermolecular bonds due to crosslinking procedures in a mixture of  $\text{CaCl}_2$ /boric acid crosslinking solution. The much stable membranes exhibited an increase in mechanical stiffness and strength with crosslinking time due to the formation of a more closely packed molecular structure of the blend PVA/SA films. In general, the scientific understanding of this thesis work involves the ability to crosslink PVA/SA membranes in  $\text{CaCl}_2$ /boric acid solutions and the structure-property relationships of the crosslinked PVA/SA membranes.

In addition to the scientific findings on the physicochemical properties of the crosslinked blend PVA/SA membranes, this thesis work provides the engineering application that PVA/SA membranes have the potential to become a multipurpose topical

dressing material. Our results suggested that the structure-property relationships of PVA/SA membranes depended on the crosslinking time, and hence, a variable to use for adjustment of the dissolution rate of the PVA/SA membranes. Presently, drug delivery from topical dressings is achieved by using a gel and/or cream matrix. The burst release behavior (liquid-based transport phenomenon) and the low dosage capability are the drawbacks for the gel and/or cream drug delivery platform. The current thesis work demonstrated that PVA/SA membranes are one of the potential candidates in solid formulation for drug delivery. The ability to utilize diffusion as well as dissolution to facilitate drug release, through the control of crosslinking of the PVA/SA membranes, is a significant improvement for the development of “tailor-made” topical dressing materials.

## Chapter 3: Literature Review

Wound healing is a dynamic cellular process, consisting coagulation and hemostasis, inflammation, migration and proliferation, and remodeling phases, where the optimal outcome is the recovery of the anatomic integrity and biological function. The prime objective of wound dressings is to manage wound conditions, or to deliver wound healing agents from novel wound dressings, to allow speedy and full healing without spreading infection and sepsis [12]. The extracellular matrix, growth factors, and cytokines play a main role in the wound healing continuous process. Later, the use of sodium alginate (SA) and polyvinyl alcohol (PVA) in wound dressings and their functions in wound healing will be reviewed to support the current thesis study. Thus, this chapter provides significant scientific understanding of the biological aspects of wound healing and the engineering applications in medical performance of novel wound dressing.

### *3.1 Wound healing stages*

A typical wound healing process comprises four overlapping and time dependent stages, which are categorized as hemostasis, inflammation, proliferation, and remodeling phases [13,14]. A normal wound follows these healing steps for tissue regenerations and/or repairs, while a delay or an incomplete stage results in non-healing wounds.

Hemostasis and coagulation occur in the first stage of the wound healing process that takes place immediately at the time of the injury, and it is completed within hours, depending on the severity of the wound. Shortly after the skin injury, the bare sub-endothelium, tissue factor, and collagen will trigger platelet aggregation resulting on the

degranulation and delivering of chemotactic factors (chemokines) and growth factors (GFs) to assemble the clot [15]. Furthermore, the clot is attained through three key mechanisms, namely (1) contact pathway, (2) tissue factor pathway, and (3) platelet activation. In contact pathway, the endothelial damage exposes the sub-endothelial tissue to blood, which trigger the Factor XII (Hageman factor). This incident starts a sequence of events as Factor X converts prothrombin to thrombin that derives into fibrinogen, where fibrinogen transforms to fibrin that generates the fibrin plug. In tissue factor pathway, the endothelial damage lays bare the tissue factor to blood, and this event generate the activation of Factor VII which also contributes to the thrombin generation. In platelet activation, the morphology of platelet suffers a change with the activation by thrombin allowing the activate platelets plug and stop the bleeding [16]. The clots serve as a matrix for immune cells in the subsequent stages of tissue repair and wound healing [17], as shown in Figure 3 [18].

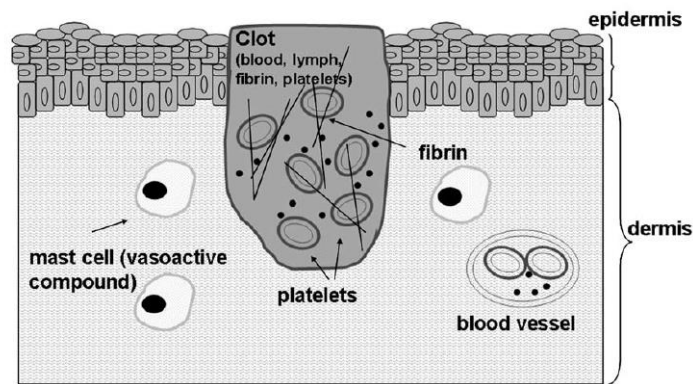


**Figure 3.** The interactions between platelets, blood, lymph, and fibrin cause the formation of blood clots during the hemostasis and coagulation stage [18].

The second phase of the wound healing process is the inflammatory stage, which is initiated during hemostasis and coagulation phase with a duration of approximately two days [7,19]. The platelets, set up by the inflammation process, promote the intrusion of leukocytes by releasing cytokines and growth factors (e.g., IL-1 $\alpha$ , IL-1 $\beta$ , IL-6 and TNF- $\alpha$ ) [17]. The main purpose of the inflammation stage, consisting of an initial and late inflammatory phase, is to prevent infections to the wound site [16,20,21]. During the initial inflammatory phase, the neutrophils infiltrate in the wound site and start the phagocytosis process in order to eradicate bacteria. More importantly, phagocytotic function is decisive for the overall healing process since a bacterial imbalance is a detriment for an optimal healing outcome [13,16]. In the late inflammatory phase, the macrophages present in the wound continue the phagocytosis process [13]. The degrading neutrophils in combination with the wound fluids consisting of denatured tissue create the wound exudate that moisture and protect the newly formed tissues, as shown in Figure 4 [18]. The inflammatory phase is a crucial step in wound healing due to its involvement on prevention of infection to promote tissue regeneration [22].

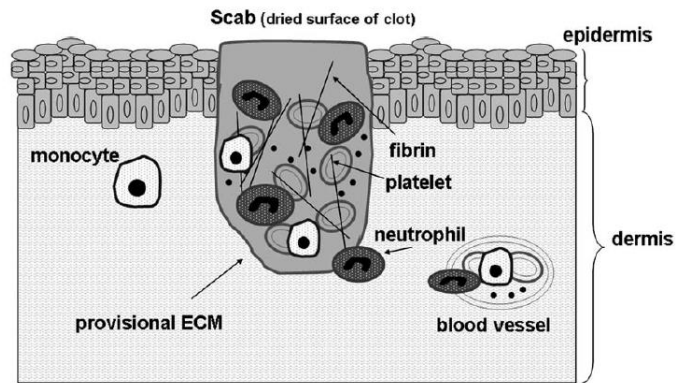


**Figure 4.** During the inflammation stage, leukocytes and monocytes migrate into the wound, where chemoattractants for neutrophils are released from damage tissue as the mediators [18].

Since the presence of growth factors and cytokines delivered by the immune cells during the inflammation stage provokes cell proliferation [21], the proliferation phase, approximately 3-10 days after the injury, becomes the third phase in wound healing. The fundamental functions of cell proliferation in wound healing include wound closure, granulate tissue formation, and reconstruction of the vascular network [17,23]. Throughout the proliferation stage, the damage tissues are gradually replaced with the granulate tissues, consisting of macrophages, fibroblasts, and vascular endothelia cells, as shown in Figure 5 [18]. Also, in this stage, a provisional extracellular matrix, assembled from vimentin, fibronectin, vitronectin, and mucin, triggers cell migration, proliferation, and cell adhesion [24]. Of equal importance, keratinocyte growth factor (KGF), EGF, TGF $\alpha$ , wound fibroblasts, and wound macrophages promote the migration of epidermal cells to the wound and their proliferation while also contributing to the synthesis of extracellular matrix [17,18].

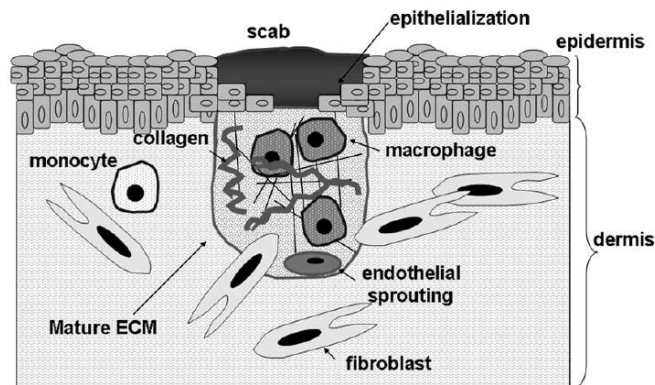


**Figure 5.** During the proliferation phase, endothelials sprout and granulate, whereas fibroblasts and collagen contribute to the formation of a mature extracellular matrix (ECM) [18].

Remodeling is the last phase of wound healing with processing times ranging from 21 days to a year or more depending on the severity of the injury. In this stage, three major events occur, including (1) the formation and degradation of scar tissues, (2) the remodeling of fibroblasts to myofibroblasts, and (3) the formation of the collagen extracellular matrix from the previous provisional extracellular matrix. In the first event, the formation of the scar tissue prevents tissue dehydration and infection at the wound site [25]. However, scar tissues are fibroblasts and/or myofibroblasts that have different cell morphologies and cell responses than the normal skin epithelial cells. In the second event, infiltration of fibroblasts in the wound site during the transition from inflammation to proliferation stage accumulates collagen. The migration of fibroblasts and their proliferation lead to angiogenesis, a complex cell remodeling process based on the interactions between the extracellular matrix and the mediators, as shown in Figure 6 [18,26]. In the third event, the provisional extracellular matrix is replaced by the collagen

extracellular matrix, setting up the fading of the inflammatory phase [17]. The evolution from the extracellular matrix to scar tissues requires the remodeling of the connective tissue of the wound. As a result, extracellular matrix maturation during remodeling promotes the reorganization, strengthen, and thickening of the epidermis by downregulating cellular and vascular content of the extracellular matrix [18].

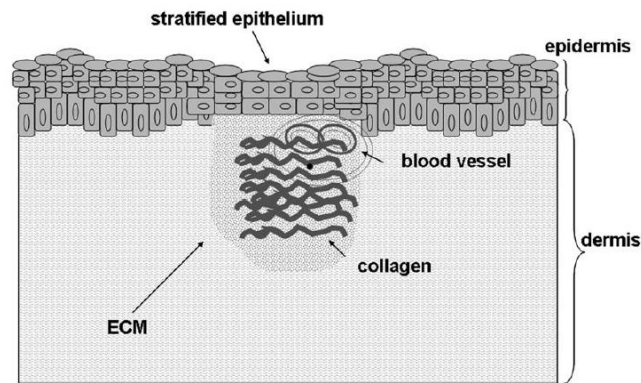


**Figure 6.** Remodeling and maturation of the extracellular matrix (ECM) foment the diminishing of collagen, cellular, and vascular contents within the ECM and promoting the thickening of epidermis as the epithelium stratifies [18].

### 3.2 Topical dressings for wound healing

The human skin is the largest visible organ and its function is to defend the body against shocks, bugs, and microbes. The recovery from a wound is essential to maintain the health of a human body, especially in diabetes patients [27]. Thus, an optimal wound healing requires a treatment capable of balancing the complex series of functions between cell types, cytokine mediators, and extracellular matrix [28].

The quick restoration of the skin integrity is crucial due to the skin important part on a variety of vital functions, as preventing infections and fluid loss [29]. An acute

wound usually heals in an orderly manner. As soon as the blood is spilled on the site of the injury, the platelets meet with the exposed collagen and various extracellular components. This contact generates reactions that release clotting factors, growth factors, platelet-derived growth factor (PDGF), and transforming growth factor beta (TGF- $\beta$ ) within the wound. The following phagocytosis process removes alien materials and bacteria while releasing PDGF and TGF- $\beta$ . Once the injured zone is cleaned out, fibroblasts migrate to the wound site and begin proliferation and remodeling of the tissue structure [30].

The fundamental function of a wound dressing is to expedite the healing by covering the wound surface to create a better healing condition. Correspondingly, an ideal wound dressing should be able to maintain a moist environment, keep away infections, absorb site wound fluids and exudates, foment growth factors, and reduce and prevent surface necrosis and desiccation, respectively [31]. Furthermore, from a mechanical design point of view, a wound dressing should be elastic, biocompatible, non-antigenic, and should reduce adhesiveness with time [31,32]. Moreover, a wound dressing can deliver a wide variety of therapeutic agents, such as small molecule drugs, growth factors, nucleic acids, or cells [33].

A large number of wound dressings have been developed due to the diversity of wounds and modes of healings. For example, the common materials used in the fabrication of wound dressings include natural polymers such as polysaccharides (alginates, chondroitin, chitin, celluloses, dextran, heparin, chitosan, gelatin, and collagen), proteoglycans, and proteins (collagen, gelatin, fibrin, keratin, and silk fibroin),

and synthetic polymers (polyurethane, poly(lactic acid), silicon rubber, and polyvinyl alcohol) [31,34]. In general, an ideal wound dressing is required to exhibit multi-purpose actions, such as moisture control, antibacterial effect, hemostasis, regeneration boost capability, to promote wound healing [35].

### *3.2.1 Biocompatibility*

A patient suffering from a chronic wound represent a lengthened healing time and costly treatment procedures. Considering the development of topical wound dressings to promote wound healing, researches have been focused on the biocompatibility of the wound dressing, which affects the functionality of the biological systems [36].

Specifically, a wound dressing should have the same physicochemical and biological qualities as the wound site with degradation by-products, if degradation/dissolution occurs, that are non-toxic to the tissues [37].

Currently, most wound dressing are formulated from biopolymers (e.g., proteins and polysaccharides), synthetic polymers (e.g., polyvinylpyrrolidone (PVP), polyvinyl alcohol (PVA), polyethylene glycol (PEG), and polyethylene (PEO)) [38], or material such as ceramic and metals [37,39]. Biopolymers or biomaterials are able to remain in contact with tissue or bodily fluid for an extended period of time with minimal secondary reactions to support wound healing [40]. The chemical structure of biomaterials can be incorporate with biological components to make them capable of being integrated with a host tissue. Therefore, biocompatibility and biofunctionality are the key factors for a biomaterial [39], and materials characterization is the best tool to make sure that these materials are harmless with living tissue [41]. Biomaterials embody a interdisciplinary

development in which natural and synthetic material are employed for a diversity of needed outcomes in a living system [41]. Hence, advances in biotechnology have enabled techniques and methods to modify the surface of biomaterials as films for drug delivery in topical applications [42].

### 3.2.2 Gels

Maintaining moisture balance of a wound has been considered for many years as the key in wound management due to its benefit in promoting cellular proliferation and in the ease of diffusion of growth factors. As a result, gels have been the main choice for wound care due to their high water content (e.g., >90%) [28]. However, in order to achieve the desired therapeutic outcome, effective wound management through moisture control at the wound site requires frequent applications of the gel dressings.

Recurring inflammation is the main result that causes chronic wounds, where the mononuclear cells present in this event destroy the healing tissue to advance the inflammation phase. To overcome the issue in recurring inflammation, a study investigated the gel formulation of using *Kaempferia marginata* Carey (Zingiberaceae family) plant for anti-inflammatory response in wound healing [29]. The anti-inflammatory properties of the reported gel were obtained from in vitro anti-nitric oxide (NO) assays by using RAW264.7 and human dermal fibroblast (HDF) cell lines. Results showed that the *K. marginata* gel (5% w/w) exhibited a cell viability of 134% with cell migration rate of 85% using HDF cells. In another study, topical gels made from 15% *Albizia amara* leaves extract and 1% carbopol displayed an enhancing wound healing effect in a model treated with this gel compared with the models treated with low,

medium extract and plain gel, and standard medication ( $P < 0.05$ ) [30]. Others investigated in the use of chitosan in gel dressing since the chemical structure of chitosan tends to form into gels in acid media. A study based on chitosan gel blend with chlorhexidine showed antibacterial ability and promotion in wound healing [43]. The histological experimentation demonstrated a greater contraction wound in an animal model on the 14<sup>th</sup> day after being treated with chitosan hydrogel containing 2% chlorhexidine compared with the control groups. Table 1 summarized studies using gels in dressing application for wound healing.

**Table 1.** Applications of topical gels in wound healing.

Gel composition	Study	Results	Ref
Chitosan and EGF	Determining the gel effect on healing of a second-degree burn in a rat model.	Chitosan/EGF gels showed a wound closure of $4.95 \pm 0.39$ after the 14 <sup>th</sup> day as compared to a wound closure of $3.10 \pm 0.68$ using chitosan only.	[44]
Collagen, chitosan, and cell-penetrating peptide (CPP)	Inhibition of <i>Staphylococcus aureus</i> and good wound healing capability in a mouse wound model.	Collagen/chitosan/CPPs gels display a wound closure of $98 \pm 4.71$ after the 14 <sup>th</sup> day as compared to a wound	[45]

(Oligoarginine, R8)		closure of $96 \pm 4.47$ using collagen/chitosan gels.
Cuttlefish skin gelatin (CSG) and aqueous henna extract (AHS)	Observation of healing and anti-inflammatory effect in a rat wound model.	CSG/AHE showed a $98.70 \pm 0.12$ wound contraction as compared to a wound contraction rate of $86.88 \pm 0.4$ using CSG gels only. [46]
Polyethylene glycol and dopa polymer-based gel	Promotion of wound healing in a mouse model contaminated with <i>Staphylococcus aureus</i> , <i>Pseudomonas aeruginosa</i> , <i>Acinetobacter baumannii</i> and <i>Clostridium perfringens</i>	After 21 days, the untreated groups remained infected while the groups treated with the gel not only achieved wound healing but also showed re-epithelialization and dermal maturation ( $P < 0.05$ ). [47]

### 3.2.3 Films

The primary function of wound dressings is to further stop tissue loss due to the worsening condition in chronic wounds, such as diabetic, decubitus, venous leg ulcers, chronic burn wounds, and traumas [48]. The main focus on designing a wound dressing is to control infection beneath the dressing. For instance, a severe burn wound requires the

application of topical antimicrobial drug [49]. Drug-incorporated wound dressings therefore have an effective role in the wound healing as they either directly or indirectly act as a cleanser and/or a carrier to include growth factor or other antimicrobial ingredients [50].

Wound dressings made from biomaterials greatly enhance the therapeutic functions due to their abilities in carry chemical and/or biological agents, such as small molecule drugs and growth factors, that can be programmed to deliver and stimulate cellular response [51,52]. In particular, the interest on the biocompatibility and biodegradability of synthetic polymers such polyvinyl alcohol (PVA), and natural polymers such alginates, starch, and chitosan has been growing over the last two decades. These polymer blends have a wide application on the pharmaceutical and biomedical field. For example, an in vitro study showed excellent antibacterial activity from the blend polyvinyl alcohol (PVA)/sodium alginate (SA) membrane loaded with ampicillin [53]. Table 2 summarized studies of various film formulations employed in wound healing.

**Table 2.** The uses of film-based dressings in wound healing.

Film composition	Study	Results	Ref
Hyaluronic acid (HA) and sodium alginate (SA) crosslinked with $\text{Ca}^{2+}$ , $\text{Zn}^{2+}$ , or $\text{Cu}^{2+}$ to	The use of an antibacterial film on albino rat wounds.	The group treated with HA/SA/ $\text{Ca}^{2+}$ films without drug received a wound contraction of $1.214 \pm 0.041$	[27]

---

<p>enhance antibacterial drug delivery of sulfadiazine (SD)/silver nanoparticles (AgNPs)</p>		<p>while drug-loaded films showed a <math>1.271 \pm 0.48</math> wound contraction over 7 days. By day 21, both groups showed 100% wound healing.</p>	
<p>Chitosan (CS), polyvinylpyrrolidone (PVP), and bentonite (BN)</p>	<p>Investigation of physical and antibacterial properties of the film using in vitro MTT assay and in vivo animal model wound.</p>	<p>The film was non-toxic to fibroblast cancer cells from MTT cytotoxicity assay. The CS/PVP/BN group showed the best healing results in a period of 16 days.</p>	<p>[54]</p>
<p>Cellulose (Cel), polyvinyl alcohol, and vitamin C or propolis (Prop)</p>	<p>Studies of in vitro- antibacterial analysis and in vivo- induced diabetic model using a cellulose-based film loaded with vitamin C.</p>	<p>The Cel/PVA groups showed a <math>460 \pm 21</math> wound closure of while the Cel/PVA/Vit C/Prop groups showed a <math>457 \pm 18</math> wound closed at day 15. The in vitro assays showed reduction of bacteria counts.</p>	<p>[55]</p>

---

Chitosan (CS), sodium alginate (SA), carbopol, and mupirocin	Studies of adhesive films for a dermal drug delivery in a wound mice model.	The control group showed wound contraction of 86.41% and 21.36% for day 4 and day 10, respectively, whereas drug-loaded groups showed 51.01% and 5.88%, respectively.	[56]
--	---	---	------

### 3.3 Sodium alginate in wound healing

One of the biomaterials that are widely utilized in wound dressing is sodium alginate (SA), which is a biocompatible natural polymer characterized by low toxicity to human tissue [57]. Alginates are natural anionic polysaccharide heteropolymers consisted of 1,4-linked  $\beta$ -D-mannuronate (M)-C5 epimer, and  $\alpha$ -L-guluronate (G) residues chains shown in Figure 7, which lay out on blocks of M, G, and the alternating domains of G/M. The carboxylate groups of the residue's chains can easily bind with metal cations forming a crosslinked hydrogel, which can be fabricated through many crosslinking methods. Among them, calcium alginate is the most ionic crosslinked hydrogel used in biomedical and food industry [58,59].

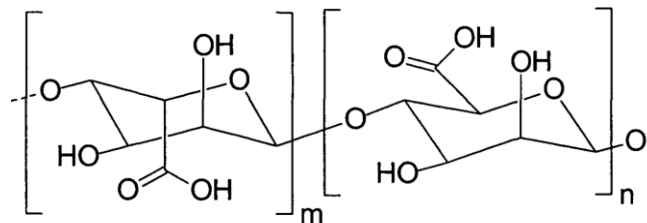


**Figure 7.** Molecular structure of alginic acid containing  $\beta$ -D-mannuronic acid (m), and  $\alpha$ -L-guluronic acid (n) residues.

In biotechnology and food industries, sodium alginate is utilized to thicken solutions and form gels. The formation of gels is the result of the interaction between the guluronate residues of adjacent alginate chains and the divalent cations (e.g.,  $\text{Ca}^{2+}$ ), illustrated in Figure 8 [60,61]. As a result, calcium alginate exhibits fast swelling and dissolution in water, and high mucoadhesiveness properties [62].

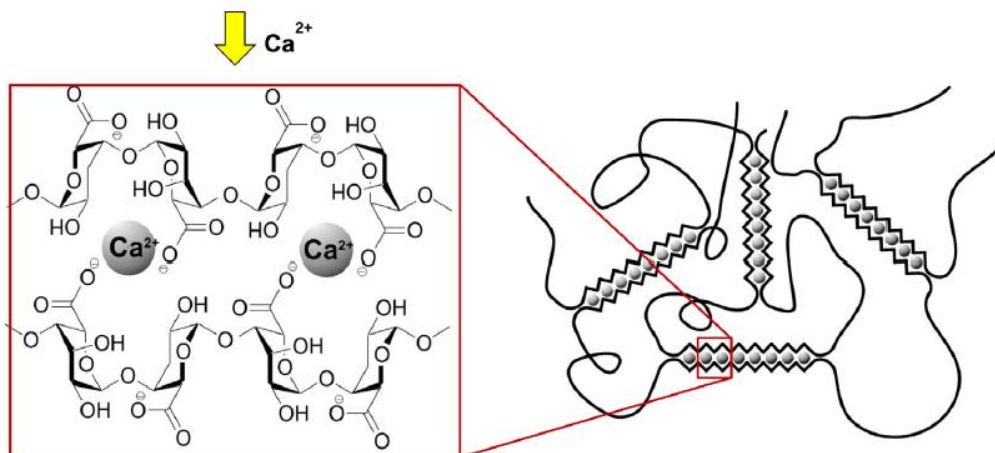


**Figure 8.** Structure of alginate and its binding of calcium cations in egg-box model [63].

Hence, alginates have been employed to fabricate hydrogels for drug delivery, tissue engineering applications, and cell transplantation and encapsulation [64], as well as

matrixes for holding and delivery biological agents [65]. Moreover, calcium alginate analogous characteristics to the extracellular matrix (ECM) in tissues has fomented its application on wound healing [66]. Table 3 summarizes studies of calcium alginate films utilized in wound healing.

**Table 3.** Alginate film-based dressings in wound healing.

Film	Study	Result	Ref
Kaltostat film	Calcium alginate (Kaltostat) and porcine xenograft films were compared in the treatment of split-thickness skin graft of 20 donors.	The healing time was 8.1 days and 11.3 days for alginate films (Kaltostat) and porcine xenograft films ( $P < 0.001$ ).	[67]
Calcium alginate film	A retrospective study of the application of alginate films in 200 circumcised newborns over two years was performed. In this study a plastibell with a calcium alginate dressing was utilized on this procedure.	This method of circumcision did not have bleeding complications like previous years. The delayed rate separation of the bell was 2.9 % on this study compared to 2.5% of the previous data.	[68]

Calcium alginate film	This study consisted of calcium alginate dressings application on burn wounds for a period of 12 years in the Women's and Children Hospital burn unit.	Calcium alginate films reduced infections rate, with a good hemostasis and satisfactory healing of the burn wound.	[69]
Calcium alginate film	The healing properties of calcium alginate film applied on a diabetic ulceration of a model rat were observed in this study.	The expression of collagen I/III for the alginate groups was from day 7 ( $1.07 \pm 0.31$ vs $0.77 \pm 0.11$ , $P < 0.05$ ) to day 14 ( $1.18 \pm 0.30$ vs $0.83 \pm 0.14$ , $P < 0.05$ ) greater than for the Vaseline groups. Alginate group displayed a high-level of the hydroxyproline in skin homogenate.	[70]

### 3.4 Polyvinyl alcohol (PVA) in wound healing

Polyvinyl alcohol (PVA) is a semi-crystalline bioadhesive polymer with a wide application in the medical field [71,72]. PVA is a hydrophilic polymer with dehydration properties by evaporation [73]. Made from polyvinyl acetate through hydrolysis [74], PVA is a super synthetic macromolecule that exhibits superior biodegradability with a

great film forming ability and mechanical properties, and its molecular structure is shown in Figure 9 [75].

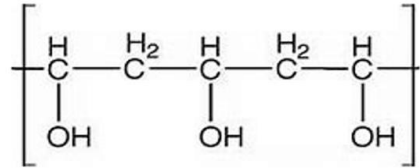


**Figure 9.** Molecular structure of polyvinyl alcohol with repeating monomer of  $\text{CH}_2\text{CHOH}$ .

PVA possesses a high value of elongation at break and average mucoadhesive properties [62]. Even though PVA has excellent chemical resistance and physical properties in dry condition, its high solubility in water affects its application. However, crosslinking methods can modify PVA's hydrophilicity condition. PVA membranes have been utilized in many applications in the biomedical and biochemical fields due to their biocompatibility, biodegradability, and permeability [76]. In the field of tissue engineering, PVA membranes have been employed to repair and regenerate tissue including mimicking corneal, arterial, and cartilage implants [77]. PVA's presence in polymer blends contributes to change the permeability of gases, enhancement of processability, increase of thermal and mechanical resistance, regulation of swelling, and ability to stabilize polymeric matrix [78]. Table 4 shows various studies of blend polymers using PVA and natural polymers and their enhanced properties.

**Table 4.** Topical film-based dressings from blend polyvinyl alcohol (PVA) and natural polymers.

Blend and drug	Enhance property of the film	Ref.
Wound dressings from blends of PVA/calcium alginate at 10, 20, and 30% v/v loaded with papain.	FTIR-ATR analysis displayed molecular structure interaction between PVA and calcium alginate. The addition of calcium alginate added softness without altering the ductility of a pure PVA film, an improved quality for wound dressing. Papain release displayed hemolytic activity from the blend films.	[78]
Burn wound dressings from blends of PVA/chitosan	Elongation at break of the films decreased as increasing PVA content or decreasing chitosan. Tensile stress of PVA/chitosan films increased minimally with decreasing chitosan content. The antibacterial property increased due to the addition of chitosan in blend.	[79]
Wound dressings from blends of PVA/silk sericin	X-Ray photoelectron spectroscopy showed the molecular blending of PVA with sericin formed hydrogen bonds that increased the mechanical properties and water retention capacity of the film.	[80]

Blend of PVA/cashew gum polysaccharide to support the immobilization of trypsin inhibitors with antibacterial activity.	A homogeneous macroscopic surface without bubbles was obtained from the blend. A higher swelling percentage of the film represented a high concentration of cashew gum polysaccharide in the blend, suggesting more covalent bonds that are responsible for a higher mechanical resistance.	[81]
Wound dressings from blends of PVA/chitosan loaded with curcumin	The antioxidant and antibacterial properties of chitosan and addition of curcumin accelerated various phases of wound healing.	[82]

### 3.5 Crosslinking mechanism

Crosslinking is an important mechanism involved in the modification of an existing molecular configuration in polymers to improve the materials properties [83].

Polyvinyl alcohol (PVA) is a linear polymer attained from vinyl acetate polymerization through partial (70%) or full (100%) hydrolysis. The presence of the hydroxyl groups in PVA makes it different from another polymers with distinct properties in crystallinity, solubility, tacticity, glass transition and melting temperature, viscosity, permeability, resistance to solvents, and swelling capacity [78]. The hydroxyl groups mainly promote water solubility and create the site for the chemical modifications [84]. The presence of water molecules in PVA swells and loosens the molecular chains and results in PVA dissolution. Therefore, the adjustment of the freely available hydroxyl

groups in PVA, done through a particular crosslinking process, determines its solubility in water [83].

The common methods to crosslink PVA consist of freezing, heat treatment, irradiation, and chemical crosslinking [85]. Freezing-thawed crystallization involves in cooling to  $-20^{\circ}\text{C}$  and thawing to room temperature many times of a dilute aqueous PVA solution. This method builds up a stable hydrogel crosslinked by the presence of crystalline regions. This technique is non-toxic and is suitable for biomedical applications [86]. In heat treatment, the PVA is usually heated to a temperature between  $120^{\circ}\text{C}$  –  $175^{\circ}\text{C}$  for around 30 – 80 minutes. Chemical bonding, unsaturation, and chain scission are the characteristics obtained from this technique [85]. Irradiation technique produces recombination of the macromolecular radicals in the polymer to give a more stable material. The new bonds, created after the irradiation procedure, are covalent linkages occurring in one single chain (intra-molecular crosslinking). Chain scissions are the rupture of the bond in the polymer backbone with double bond formation that produces new chemical groups [87].

Chemical crosslinking is usually done with a crosslinking agents or crosslinkers, such as boric acid, formaldehyde, glutaraldehyde, glyoxal, citric acid, malic acid malonic acid glycidyl sulphone, and urea formaldehyde/ $\text{H}_2\text{SO}_4$  among others [85]. In a study, PVA was crosslinked at room temperature with three concentrations of boric acid (0.3 wt%, 1wt%, and 3wt%). The results showed the correlation between the concentration of boric acid and mechanical strength of the crosslinked materials. This study suggested that increasing the content of boric acid promoted the early formation of nanofibrils followed

by a reduction of nanofibrils at the end, the coupling effect when increasing the concentration of boric acid resulted in the reduction of PVA crystallization, and the boric acid protected the PVA crystal network from breaking. Therefore, the addition of boric acid was able to modify the orientation of amorphous and crystal regions as shown in Figure 10 [84].

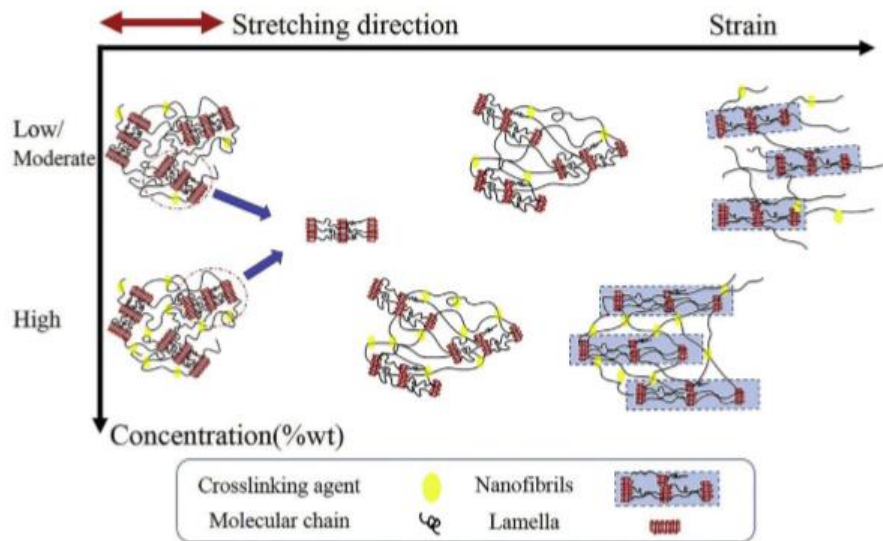


**Figure 10.** Representation of the molecular structure in PVA films during the aqueous boric acid crosslinking at different concentrations [84].

The molecular structure of alginates consists of a free number of carboxyl and hydroxyl groups allocated along the backbone of its molecular chain. As a result, alginates can be modified by chemical functionalization to obtain desirable physicochemical behaviors including the ability to swell and solubility [88]. Sodium alginate (SA) has unrestrained structure, insufficient mechanical strength, and high water solubility. Hence, research work has been focused on improving these drawbacks by

using a crosslinking procedure. Some good candidates to crosslink SA include calcium salts ( $\text{CaCl}_2$ ,  $\text{CaSO}_4$ , and  $\text{CaCO}_3$  among others) due to the ability of SA to bind divalent cations of  $\text{Ca}^{2+}$  and form hydrogels, which is the most important quality of SA [89]. The formation of the hydrogel is due to the binding of guluronic residues with calcium cations that generates a three-dimensional network, best known as the egg-box model. The frequency and length of the guluronic acid residues in SA are associated with the concentration of cations required for crosslinking. The changes on these two factors modify the numbers of alginate strands that hold the egg box model. Consequently, these events change the strength of the gel network as shown in Figure 11 [90].

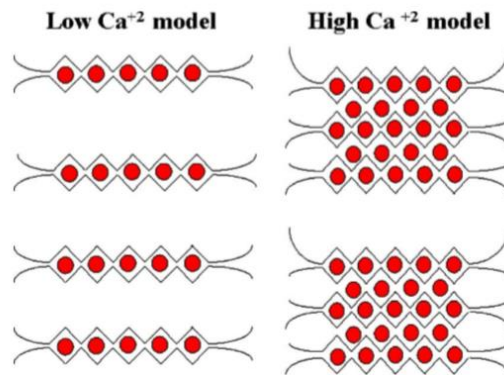


**Figure 11.** Representation of the egg-box model in low and high  $\text{CaCl}_2$  concentration.

The red solid circles depict calcium cations located between guluronic acid residues [90].

## Chapter 4: Materials and Methods

### *4.1 Materials*

Sodium alginate (SA) powder (TICA-algin<sup>®</sup> 400), kindly provided by Tic Gums (White Marsh, MD, USA), was chosen for this study based on its biocompatibility and easy formation of films with desired mechanical properties. Graded 71-30 polyvinyl alcohol (PVA) powder, kindly provided by Kuraray America Inc. (Houston, TX, USA), was used for film forming ability to blend with SA. The crosslinkers utilized in this study included calcium chloride (CaCl<sub>2</sub>) and boric acid (H<sub>3</sub>BO<sub>3</sub>) powders for SA and PVA, respectively. Deionized (DI) water was used as a solvent for polymer solutions and crosslinking procedures.

### *4.2 Preparation of polymer solutions*

To prepare 5 wt% of pure polyvinyl alcohol (PVA) solutions, 10 grams of PVA powder (Figure 12A) were added to 200 ml of DI water (Figure 12B) and stirred on a hot plate (Figure 12C) for approximately 3 hours at a temperature of 80°C. The PVA solutions were then left overnight to remove micro-bubbles due to the agitation during mixing. Sodium alginate (SA) solutions were prepared at 1 wt% (e.g., 2 grams SA powder in 200 ml of DI water) due to solubility and viscosity and stirred on a hot plate for approximately 3 hours at a temperature of 80°C. The SA solutions were also left overnight to remove the micro-bubbles from stirring processes.

To prepare the blend PVA/SA polymer solution, pre-calculated amounts of PVA and SA powders 5 wt% and 1 wt% were placed into a vial followed by adding a total of

200 mL of DI water to form a blend polymer solution. The blend polymer solutions were also left overnight for removing the air bubbles due to mixing.

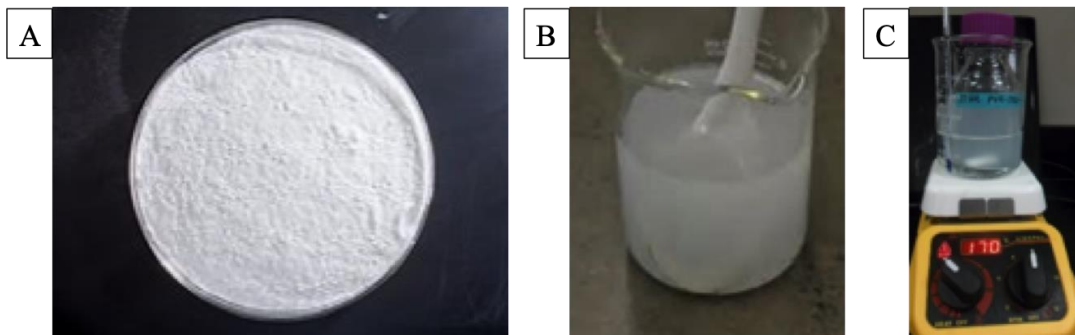


**Figure 12.** Polymeric solution making process showing (A) raw polymer powder (image represents PVA powder), (B) PVA powder in deionized water before the mixing process, and (C) solution stirring and heating process using a stirring hot plate.

#### 4.3 Fabrication of films

After removing the air-bubbles from the polymer solutions, 50 ml of solution was carefully pour down to a Teflon-coated aluminum mold (7” in diameter) followed by solvent evaporation process at 40°C for 6 hrs. After solidification, films were carefully lifted-off from the mold without additional applied stress in distortion to the films.

Representations of the solvent cast films after solidifications are shown in Figure 13 for a typical pure PVA film (Figure 13A), a typical pure SA film (Figure 13B), and a typical blend PVA/SA film (Figure 13C).

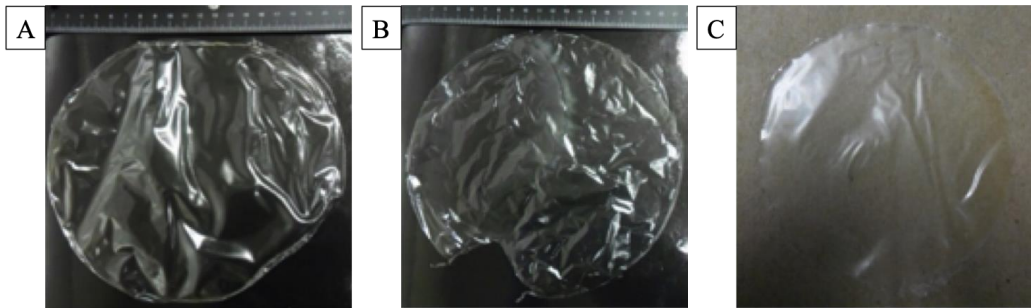


**Figure 13.** Solvent casting method for fabrication of the polymer films of (A) PVA film, (B) SA film, and (C) blend PVA/SA film.

#### *4.4 Preparation of crosslinking solutions*

The crosslinkers employed for this study were  $\text{CaCl}_2$  for SA, and boric acid for PVA. Three types of crosslinking solutions were prepared for pure PVA, pure SA, and blend PVA/SA films. Figure 14 illustrates the final products of the crosslinking solutions from 5 wt%  $\text{CaCl}_2$  (Figure 14A), 3 wt% boric acid (Figure 14B), and 50/50 volumetric mixture of  $\text{CaCl}_2$ /boric acid solution from the same weight percentages of the crosslinkers (Figure 14C). All crosslinking solutions were optically clear without residuals.

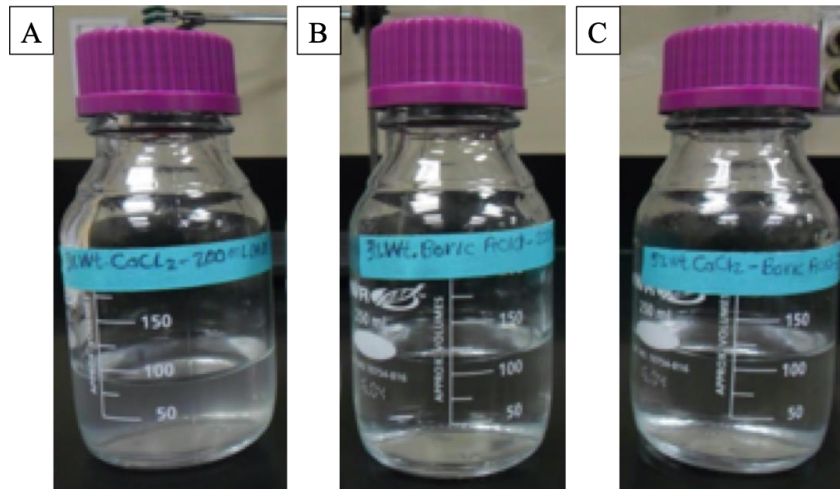


**Figure 14.** Various crosslinking solutions for pure PVA, pure SA, and blend PVA/SA films showing (A)  $\text{CaCl}_2$  solution, (B) boric acid solution, and (C) mixture of  $\text{CaCl}_2$ /boric acid solution.

#### 4.5 Crosslinking procedures

Sets of disc samples were cut using a series of hollow leather punch with diameters of 19, 16, 13, and 11 mm. Before crosslinking, the area, thickness, and weight of each sample were measured using a Hewlett-Packard scanner, a thickness gauge, and a Mettler Toledo analytical balance, respectively. The disc samples from pure PVA, pure SA, and blends of PVA/SA were fully immersed in their corresponding crosslinking agents for 5, 10, and 30 minutes. After crosslinking, the discs were removed from the crosslinking solutions and extensively washed with DI water to remove excess crosslinking agents followed by leaving them to dry at room temperature.

#### 4.6 Physical properties characterizations

The images of the PVA, SA, and PVA/SA film samples were acquired by a Hewlett-Packard Deskjet 2540 scanner. The mass of the samples was recorded by a Mettler Toledo AG245 analytical balance, 220 g x 0.1 mg instrument. The thickness of the film was measured using a digital thickness gauge from CAIDU (portable digital thickness gage gauge 0.0005-0.5-inch/0.01-12.7 mm – range electronic micrometer inch/metric – electronic percentage thickness meter with precise LCD display). The percentage changes in area (swelling/shrinkage), weight (dissolution), and thickness (diffusion), were measured and calculated for the all sample films. In particular, the scanned images were analyzed by the ImageJ software (NIH, Bethesda, Maryland).

Changes in weight, area, and thickness of sample films were analyzed after 5, 10, and 30 minutes of crosslinking in CaCl<sub>2</sub>, boric acid, and the combination CaCl<sub>2</sub>/boric acid solutions. The percentage change in area was calculate by the following equation:

$$\% \text{ Area change} = (A_f - A_i)/A_i \times 100\%$$

, where  $A_f$  is the final area of the samples after crosslinking and  $A_i$  is the initial area of the samples before crosslinking. Similarly, the percentage change in thickness was calculate by the following equation:

$$\% \text{ Thickness change} = (T_f - T_i)/T_i \times 100\%$$

, where  $T_f$  is the final thickness of the samples after crosslinking and  $T_i$  is the initial thickness of the samples after crosslinking. Finally, the the percentage change in weight was calculate by the following equation:

$$\% \text{ Weight change} = (W_f - W_i)/W_i \times 100\%$$

, where  $W_f$  is the final weight of the samples after crosslinking and  $W_i$  is the initial weight of the samples after crosslinking.

#### *4.7 Fourier-transform infrared spectroscopy*

To characterize the change in chemical structures after crosslinking, PVA/SA films before and after crosslinking in  $\text{CaCl}_2$ /boric acid solutions were prepared for Fourier-transform infrared spectroscopy at the LeTourneau University (Longview, TX, USA). Chemical analyses were performed by Attenuated Total Reflectance mode in Fourier transform infrared spectroscopy (ATR-FTIR) using a Nicolet 6700 (Thermo Fisher Scientific Inc., USA) spectrometer with a diamond crystal over a scan range from 400 to  $4000 \text{ cm}^{-1}$ .

#### *4.8 Mechanical Testing*

An Instron universal mechanical tester (Norwood, MA, USA) was used for the tensile testing of the films according to ASTM standard D5034-95 (e.g.,  $24 \pm 1 \text{ }^\circ\text{C}$  and  $45 \pm 5\% \text{ RH}$ ). Film samples were cut with dimensions of 15 mm x 5 mm (Figure 15A). For crosslinked samples, they were cut and crosslinked for 5, 10, and 30 min with their corresponding solutions. After the films dried up, they were taped with VWR lab tapes (Figure 15B) before clamping to the fixture for tensile testing.

Tensile tests were performed at a strain rate of 0.01/s. Stress-strain curves were obtained from the raw data of load and displacement from the mechanical tester. A representative stress-strain curve from the crosslinked film is shown in Figure 15C. The elastic modulus was derived from the initial slope of the stress-strain curve after tensile testing. The tensile strength represents the maximum stress that the sample can withstand,

and it is calculated by dividing the applied load to the cross-sectional area of the film, which comprises the width and the thickness of the rectangular specimen [91,92].

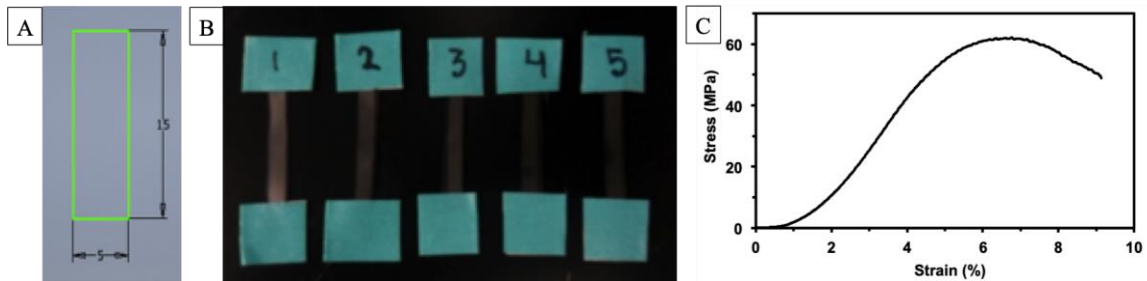


**Figure 15.** (A) Schematic of a rectangular specimen used in tensile testing (unit = mm). (B) Crosslinked set of five sample films ready for the mechanical test. Both ends of the rectangular sample films were attached to labeling tapes to enhance gripping on the mechanical tester. (C) Typical stress strain curve for a PVA/SA sample film. The representative curve was depicted from a sample crosslinked with  $\text{CaCl}_2$  for 5 minutes.

## Chapter 5: Results and Discussion

### 5.1 Physical properties PVA films

PVA membranes were prepared by heating 5 wt% of PVA solutions in an oven at 80°C for 6 h. After fully dried, the pure PVA membranes were lift-off from the cast die. The objective of this section was to investigate the changes of physical properties on solid PVA membranes after crosslinking in CaCl<sub>2</sub>, boric acid, and the combination of CaCl<sub>2</sub>/boric acid crosslinking solutions for 5, 10, and 30 minutes. The shapes of PVA discs before and after crosslinking are shown in Figure 13. Significant changes in sizes (swelling) and fold-over due to preparation processes of the crosslinking were observed. Due to the difficulties in handling the samples during crosslinking process, quantitative measurements on the changes in physical shapes of the PVA discs before and after crosslinking were not shown.

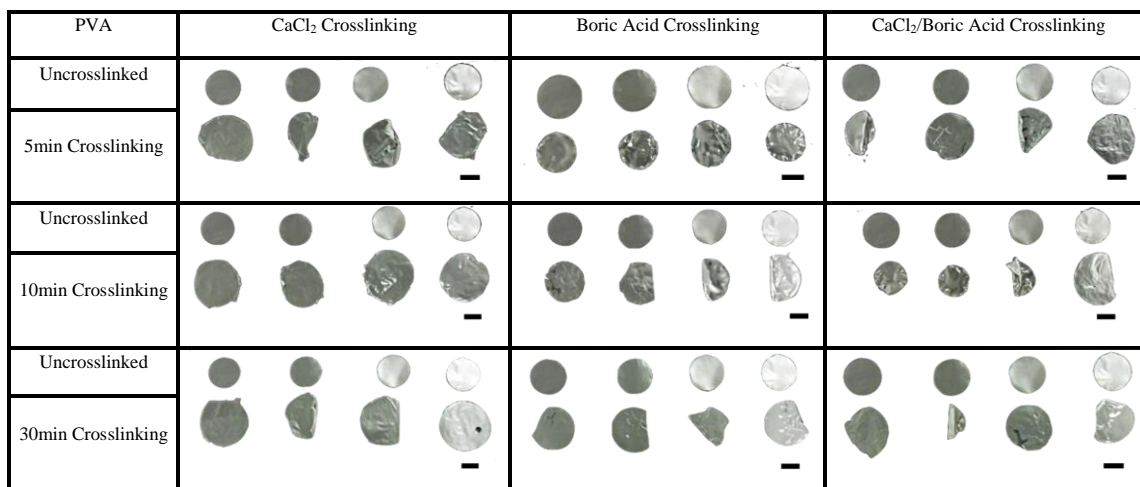


**Figure 16.** PVA sample films crosslinked for 5, 10, and 30 minutes with CaCl<sub>2</sub>, boric acid, and mixture of CaCl<sub>2</sub>/boric acid solutions. Photos depict from sample discs before and after crosslinking. Scale bars = 10 mm.

Since the quantitative measurements of disc shapes from the pure PVA samples after crosslinking were unsatisfactory, the percentage weight changes on pure PVA samples before and after crosslinking were used for quantification (Figure 14). Results show that PVA sample discs crosslinked with  $\text{CaCl}_2$  decrease 6% in weight, increases 18% in weight, and decreases 17% in weight after 5, 10 and, 30 minutes, respectively. Since the molecular chain of PVA exhibits many hydroxyl groups, a suitable crosslinking process of PVA discs requires the introduction of intra- and inter-molecule hydrogen bonds within the chains. PVA is a highly hydrophilic polymer due to the hydroxyl groups, and crosslinking of PVA using water-based crosslinkers has the potential to dissolve PVA during the process. The variation of our results from  $\text{CaCl}_2$  crosslinking at various times suggests that the hydrophilic characteristic of PVA may have impacted the measurement of the weight loss of the films. PVA sample discs crosslinked with boric acid show a slight increase in weight of 3% after 5 minutes followed by a 3% decrease of weight change at 30 minutes. The change in weight is insignificant as compared to the  $\text{CaCl}_2$  crosslinker, and therefore, boric acid appears to be a good candidate for crosslinking pure PVA. Studies suggested that boric acid accumulation on the PVA films caused a high crosslinking density that reduced its volume [93]. This mechanism suggests the minimal change in weight loss while significantly reducing the disc size during the crosslinking procedure.

PVA sample discs crosslinked with combination of  $\text{CaCl}_2$ /boric acid solutions show a weight change (e.g., increase and decrease) within 1% after 5, 10, and 30 minutes.

This result demonstrated that CaCl<sub>2</sub>/boric acid combination balance fluctuations on mass loss on a PVA film.

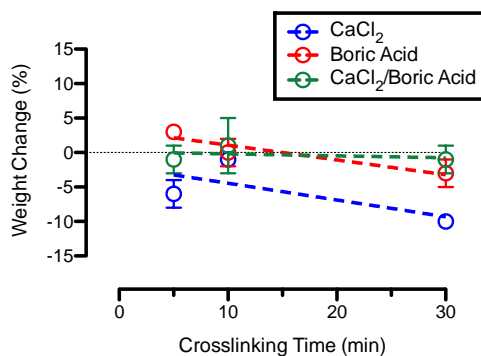


**Figure 17.** Percent weight change of PVA sample films crosslinked with CaCl<sub>2</sub>, boric acid, and mixture of CaCl<sub>2</sub>/boric acid solutions for 5, 10, and 30 minutes.

## 5.2 Physical properties of SA films

SA membranes were prepared by heating the 1 wt% SA solutions in an oven at 80°C for 6 h. The purpose of this study was to explore the physical properties of the SA membranes before and after crosslinking for 5, 10, and 30 min in CaCl<sub>2</sub>, boric acid, and the combination of CaCl<sub>2</sub>/boric acid crosslinking solutions for 5, 10, and 30 minutes. Since SA films dissolved in boric acid crosslinking solutions, the film samples were only crosslinked with CaCl<sub>2</sub> and the combination CaCl<sub>2</sub>/boric acid solutions. The physical shapes of SA film samples were distorted and exhibited significant fold-over after the crosslinking process of 5, 10, and 30 minutes (Figure 14). As such, quantitative measurements on the changes in physical shapes of the SA films before and after crosslinking were not shown.

SA	CaCl <sub>2</sub> Crosslinking	Boric Acid Crosslinking	CaCl <sub>2</sub> /Boric Acid Crosslinking
Uncrosslinked		N/A	
5min Crosslinking			
Uncrosslinked		N/A	
10min Crosslinking			
Uncrosslinked		N/A	
30min Crosslinking			

**Figure 18.** SA sample films crosslinked for 5, 10, and 30 minutes in CaCl<sub>2</sub>, boric acid, and mixture of CaCl<sub>2</sub>/boric acid solutions. Photos depict from sample films before and after crosslinking. SA dissolved in boric acid, and therefore, no images for the comparison. Scale bars = 10 mm.

Changes in weight percentage were recorded for quantification measurements before and after crosslinking process. Results suggested that SA film samples crosslinked with CaCl<sub>2</sub> for 5 minutes received a weight increase of 5% followed by a 4% decrease in weight after 10 minutes and a 2% increase in weight after 30 minutes (Figure 16). The effects of CaCl<sub>2</sub> crosslinking resulted in the rearrangement of the hydroxyl and carboxyl groups in the SA molecular chain with the formation of calcium alginate polymer [94]. Likewise, the films crosslinked with combination of CaCl<sub>2</sub>/boric acid solutions for 5 minutes showed a 2% weight decrease. After 10 minutes of crosslinking, the decrease in weight of SA sample films remained at 2%. After 30 minutes of crosslinking, the SA sample films showed a 1% weigh increase. Even though SA samples dissolved in boric

acid solution, crosslinking of SA samples in combination of CaCl<sub>2</sub>/boric acid solutions suggested minimal dissolution of the alginate.

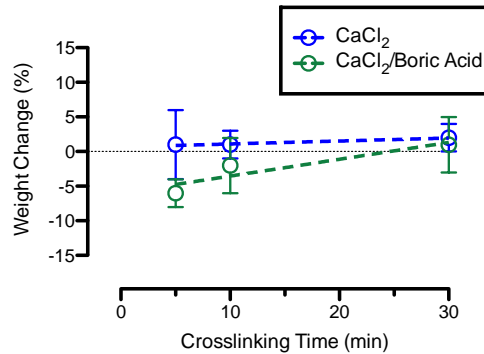


**Figure 19.** Percent weight change of SA sample films crosslinked with CaCl<sub>2</sub> and mixture of CaCl<sub>2</sub>/boric acid solutions for 5, 10, and 30 minutes. SA sample films crosslinked with boric acid were dissolved, and therefore, data were excluded.

### 5.3 Physical properties of blend PVA/SA films

Blend PVA/SA films were prepared by heating the mixed solutions of 5 wt% PVA and 1 wt% SA solutions in an oven at 80°C for 6 h. Blend PVA/SA samples were crosslinked with CaCl<sub>2</sub>, boric acid, and combination of CaCl<sub>2</sub>/boric acid solutions for 5, 10, and 15 minutes. The purpose of investigating polymer blends is to enhance the crosslinking results of physical properties on the films. All blend samples survive the crosslinking processing of the various crosslinking methods. Qualitative results on the physical shapes of PVA/SA discs before and after crosslinking in all three crosslinking solutions suggested the improvement in retaining the original shapes of the films (Figure 17). The blend PVA/SA films have a high hydrophilicity that limit wound secretions, which is an essential barrier property for wound dressings [95].

PVA/SA	CaCl <sub>2</sub> Crosslinking	Boric Acid Crosslinking	CaCl <sub>2</sub> /Boric Acid Crosslinking
5min Crosslinking			
Uncrosslinked			
10min Crosslinking			
Uncrosslinked			
30min Crosslinking			
Uncrosslinked			

**Figure 20.** PVA/SA sample films crosslinked for 5, 10, and 30 minutes in CaCl<sub>2</sub>, boric acid, and mixture of CaCl<sub>2</sub>/boric acid solutions. Photos depict from sample films before and after crosslinking.

Many chemical reactions took place during the crosslinking process of PVA/SA films (Figure 18). For instance, the effects of boric acid crosslinking on PVA/SA film samples after 5 minutes increased the area for 37%, decreased the thickness for 12%, and increased the weight for 1%. After 10 minutes of crosslinking in boric acid, the PVA/SA film samples decreased the area for 16%, increased the thickness for 15%, and increased the weigh fort 5%. Furthermore, crosslinking in boric acid solutions for 30 minutes increased the area for 12%, decreased the thickness for 4%, and decreased the weight for 3%. To interpret these results, the high solubility of SA [96], the swelling characteristic of PVA [97], and the concentration of boric acid on crosslinking of PVA increased the crosslinking density and created a consolidated packing of its molecular chains [93].

Similarly, the responses of the physical properties of the PVA/SA films after  $\text{CaCl}_2$  crosslinking (Figure 18) for 5 minutes suggested an increase of 13% in area, a decrease of 14% in thickness, and an increase of 3% in weight. Crosslinking of the PVA/SA samples in  $\text{CaCl}_2$  for 10 minutes increased the area by 14%, decreased the thickness by 12%, and increased the weight by 3%. Furthermore, crosslinking of the PVA/SA samples in  $\text{CaCl}_2$  for 30 minutes decreased the area for 4%, increased the area for 1%, and decreased the weight for 5%. Since SA comprises numerous hydroxyl and carboxyl groups in its molecular chains, the crosslinking process with  $\text{CaCl}_2$  forms calcium alginate polymer with the capacity of carry a high-water content [94].

Conversely, PVA molecular chains have only hydroxyl groups. During  $\text{CaCl}_2$  crosslinking, hydrogen bonds are formed intra- and inter-molecularly, giving a high mechanical strength to PVA. As such, PVA/SA membranes crosslinked with  $\text{CaCl}_2$  produce films with good stability, flexibility, and minimal changes in water content. The film samples crosslinked with combination of  $\text{CaCl}_2$ /boric acid solutions (Figure 18) exhibited a 16% decrease in area, a 1% decrease in thickness, and a 7% increase in weight after 5 minutes. After crosslinking for 10 minutes, the area decreased 16%, the thickness increase of 22%, and the weight increased 7%. Sample physical properties after crosslinking for 30 minutes showed a decrease in area of 21%, an increase of thickness of 68%, and a decrease in weight of 4%. In this study, it was anticipated that there was some degree of SA dissolution during crosslinking due to the presence of boric acid in the crosslinking solutions. Sample swelling and shrinkage effects due to the loss of SA in PVA/SA samples were addressed according to the literature [98].

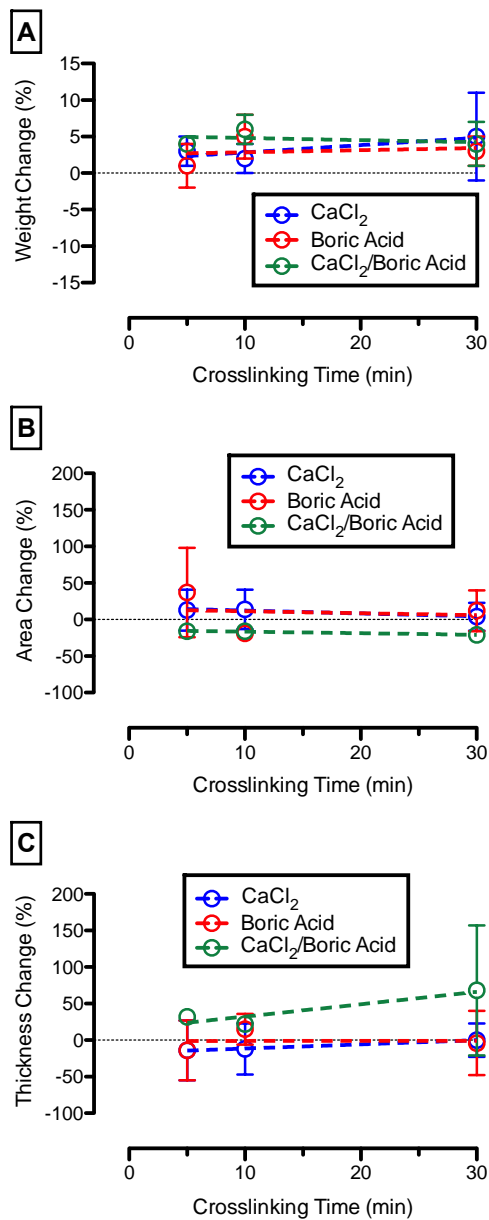


**Figure 21.** PVA/SA sample films crosslinked with CaCl<sub>2</sub>, boric acid, and mixture of CaCl<sub>2</sub>/boric acid solutions for 5, 10, and 30 minutes, showing (A) percentage weight change, (B) percentage area change, and (C) percentage thickness change.

#### 5.4 Chemical analyses: FTIR

The changes in molecular structure of the blend PVA/SA films before and after crosslinking were characterized by Fourier-transform infrared (FTIR) spectroscopy from  $500\text{ cm}^{-1}$  to  $4000\text{ cm}^{-1}$  wavenumbers. Figure 19 shows the characteristics peaks observed on the uncrosslinked blend PVA/SA films as well as the crosslinked blend PVA/SA films with  $\text{CaCl}_2$  and boric acid for 5, 10, and 30 minutes. Table 5 depicts the peak assignment for the uncrosslinked and crosslinked PVA/SA films. It was observed that hydroxyl peaks are broader due to the formation of hydrogen bonding between the hydroxyl groups of PVA and sodium alginate [99]. Moreover, all the PVA/SA films showed an increase in the (O-H) and (C=O) absorption bands when increasing the crosslinking time with  $\text{CaCl}_2$  due to the formation of calcium alginate through  $\text{Ca}^{2+}$  ions [100]. Also, an increase in the intensity of the C-H stretching was noted on the PVA/SA films after crosslinking with  $\text{CaCl}_2$  for 30 minutes.

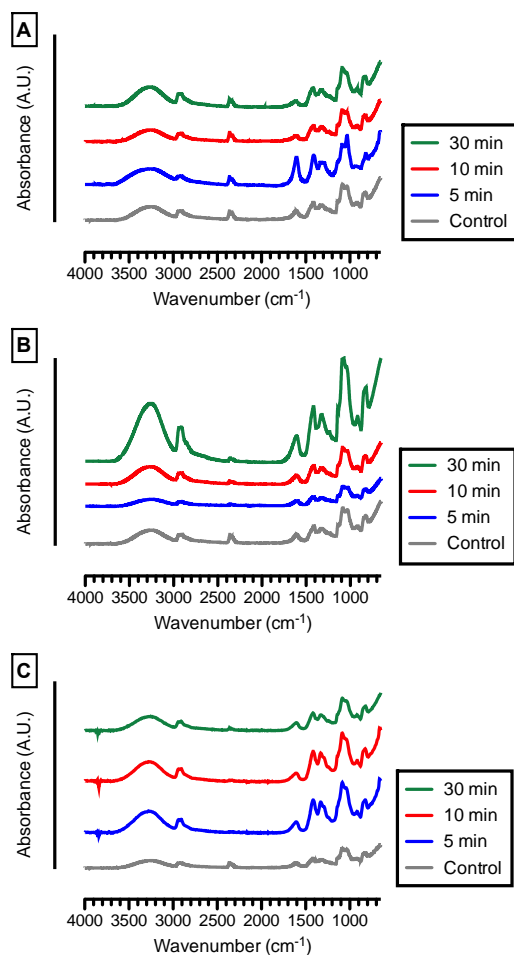


**Figure 22.** FTIR spectra of uncrosslinked PVA/SA sample films (blank) and crosslinked PVA/SA sample films with (A) boric acid, (B) CaCl<sub>2</sub>, (C) and CaCl<sub>2</sub>/boric acid solutions for 5, 10, and 30 minutes.

**Table 5.** Characteristics peaks observed on crosslinked PVA/SA films with CaCl<sub>2</sub> and boric acid for 5, 10, and 30 minutes and a PVA/SA blank film.

FTIR peak assignments on PVA/SA sample films				
Crosslinking time	Samples	Wavenumber (cm <sup>-1</sup> )		
		C=O stretching	C-H stretching	O-H stretching
5 minutes	Blank	1616	2916	3264
	CaCl <sub>2</sub>	1578	2836	3253
	Boric acid	1608	2921	3293
10 minutes	Blank	1618	2931	3260
	CaCl <sub>2</sub>	1614	2913	3275
	Boric acid	1638	2891	3199
30 minutes	Blank	1619	2914	3296
	CaCl <sub>2</sub>	1615	2933	3283
	Boric acid	1621	2898	3244

### 5.5 PVA-SA Mechanical Properties

Uniaxial tensile tests were performed on crosslinked PVA/SA samples. Five rectangular shape PVA/SA samples were used for tensile test to evaluate the changes in elastic modulus and the tensile strength due to crosslinking. Quantitative results on the elastic modulus and tensile strength of the crosslinked PVA/SA films are shown in Figure 20 and summarized in Table 6.

The average elastic moduli of PVA/SA films crosslinked with the CaCl<sub>2</sub> solutions for 5, 10, and 30 minutes were 1364 MPa, 2051 MPa, and 1956 MPa, respectively. The average tensile strength of PVA/SA films crosslinked with the CaCl<sub>2</sub> solutions for 5, 10, and 30 minutes were 47 MPa, 62.7 MPa, and 62.4 MPa, respectively.

Similarly, the average elastic moduli of PVA/SA films crosslinked with boric acid solutions for 5, 10, and 30 minutes were 1990 MPa, 1587 MPa, and 1393 MPa, respectively. The average tensile strength of PVA/SA films crosslinked with boric acid solutions for 5, 10, and 30 minutes were 63.0 MPa, 65.5 MPa, and 50.0 MPa, respectively.

Finally, the average elastic moduli of PVA/SA films crosslinked with the combination of CaCl<sub>2</sub>/boric acid solutions for 5, 10, and 30 minutes were 2151 MPa, 1899 MPa, and 2257 MPa, respectively. The average tensile strength of PVA/SA films crosslinked with the combination of CaCl<sub>2</sub>/boric acid solutions for 5, 10, and 30 minutes were 48.0 MPa, 73.8 MPa, and 77.9 MPa, respectively.

The general trends on average elastic modulus and the tensile strength after crosslinking of the blend PVA/SA films increased after crosslinking with the all crosslinking solutions. Many factors needed to take in consideration to explain this result. Most importantly, alginate is highly soluble in boric acid, and thus, it was expected that the initial composition of the blend PVA/SA film suffered a modification during the crosslinking process involving boric acid. This effect may have resulted in the leaching of polymers leaving some level of microporosity in the films. Studies have shown that the

tensile strength and the elongation at break of the blend PVA/SA membranes was a variable of the content of alginate in the film [8].

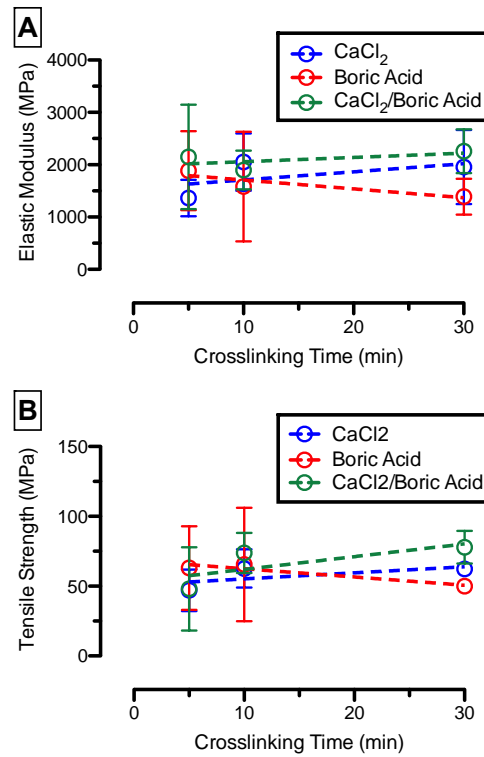


**Figure 23.** Mechanical properties of PVA/SA films, showing (A) average elastic modulus and (B) average tensile strength after crosslinking in CaCl<sub>2</sub>, boric acid, and the mixture of CaCl<sub>2</sub>/boric acid solutions for 5, 10, and 30 minutes.

**Table 6.** Mechanical properties of PVA/SA films crosslinked in CaCl<sub>2</sub>, boric acid, and mixture of CaCl<sub>2</sub>/boric acid solutions for 5, 10, and 30 minutes.

Mechanical properties crosslinked PVA/SA sample films			
Crosslinking time	Samples	Elastic Modulus (MPa)	Tensile Strength (MPa)
5 minutes	CaCl <sub>2</sub>	1364 ± 347	47.0 ± 14.9
	Boric acid	1990 ± 753	63.0 ± 30.0
	Combo	2151 ± 998	48.0 ± 29.8
10 minutes	CaCl <sub>2</sub>	2051 ± 548	62.7 ± 13.7
	Boric acid	1587 ± 1045	65.5 ± 40.6
	Combo	1899 ± 370	73.8 ± 14.4
	CaCl <sub>2</sub>	1956 ± 707	62.4 ± 2.5
30 minutes	Boric acid	1393 ± 342	50.0 ± 3.4
	Combo	2257 ± 417	77.9 ± 11.7

### *5.6 Effects of solvent-casting variables on mechanical properties*

To evaluate the feasibility in solvent casting and crosslinking of PVA and SA, our results in the previous sections demonstrated the ability to synthesize and crosslink pure PVA, pure SA, and blends of PVA/SA membranes for potential applications in wound dressings. Crosslinking of the various membranes were carried in pure CaCl<sub>2</sub> for SA, pure boric acid for PVA, and a mixture of CaCl<sub>2</sub>/boric acid solution for blend PVA/SA membranes. Significant changes in the physical shape and mass were found in the pure PVA and SA films as compared to a rather stable behavior from the blend PVA/SA films.

Thus, based on the findings observed, a decision was made to focus on studying the physico-mechanical properties of blend PVA/SA films using a mixture of  $\text{CaCl}_2$ /boric acid solution as the crosslinking agent for solvent casting and crosslinking.

Moreover, the data from the previous sections suggested that thickness of the film played an important role in the mechanical properties of the films. As a result, the aim is to standardize thickness in blend PVA/SA films to improve the characterizations of their physico-mechanical properties. One approach in standardizing film thickness is to adjust the concentrations of polymer solutions by allowing more polymers to solidify in the mold. Therefore, the following sections will focus on the discussion of effects of film thickness on physico-mechanical properties of blend PVA/SA films using different concentrations of polymer solutions. The objective of this approach is to find a polymeric blend PVA/SA film with optimal physico-mechanical properties intended for the use of a wound dressing.

### *5.7 Physical properties of blend PVA/SA films*

Three blends of PVA/SA films were prepared in an oven at  $40^\circ\text{C}$  for 6 hours by using different concentrations of PVA and SA solutions. Afterward, the blend PVA/SA films were crosslinked with a mixture of  $\text{CaCl}_2$ /boric acid solution for 5, 10, and 30 minutes. The quality of the resulting physical shapes of the PVA/SA samples after crosslinking was enhanced, as shown in Figure 21. Minimal shape changes and distortions were observed on their physical appearances, which made blend PVA/SA a good candidate in wound dressing.

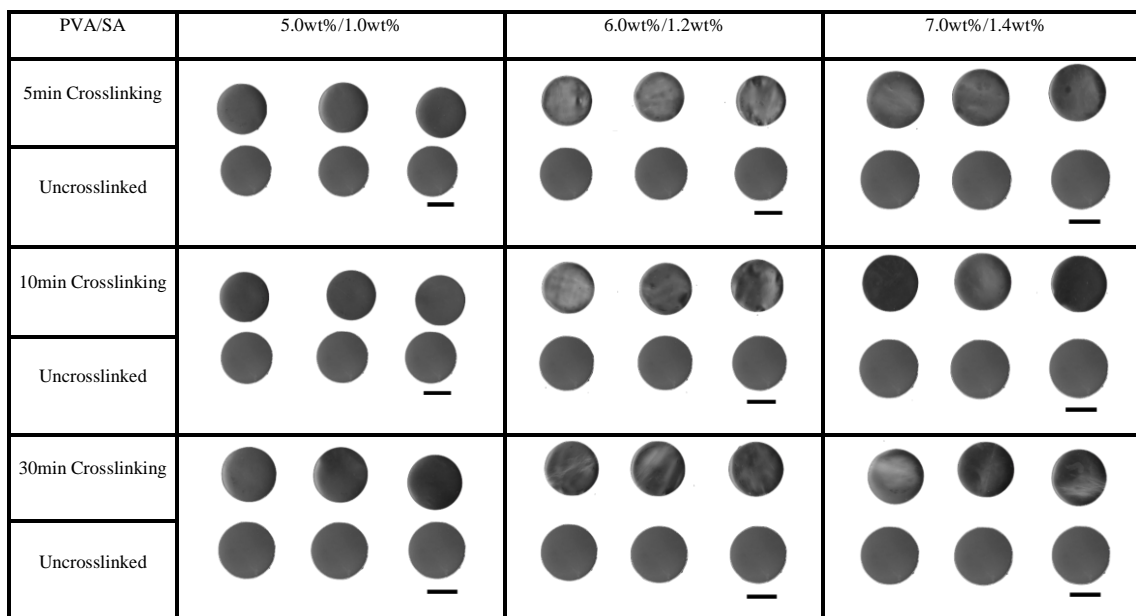


**Figure 24.** PVA/SA sample films crosslinked for 5, 10, and 30 minutes in mixture of  $\text{CaCl}_2$ /boric acid solutions. Photos show from sample films before and after crosslinking.

Quantitative analysis of the physical properties of PVA/SA films (5wt%/1wt% blend) showed that there was a slight decrease of  $0.62 \pm 0.13\%$  in weight after 5 minutes of crosslinking followed by a reduction of  $0.78 \pm 0.23\%$  and  $0.22 \pm 0.26\%$  in weight after 10 and 30 minutes of crosslinking, respectively (Figure 22A). The PVA/SA films (6wt%/1.2wt% blend) showed slight increases of  $0.04 \pm 0.06\%$ ,  $0.33 \pm 0.33\%$ , and  $1.96 \pm 0.27\%$  in weight after 5, 10, and 30 minutes of crosslinking, respectively. Furthermore, the PVA/SA films (7wt%/1.4 wt% blend) underwent increases of  $1.37 \pm 0.18\%$ ,  $1.05 \pm 0.46\%$ , and  $2.04 \pm 0.35\%$  in weight after 5, 10, and 30 minutes of crosslinking, respectively. Overall, the percentage weigh change was minimal for all three blends of PVA/SA samples. This is perhaps due to the effects that boric acid decreases the PVA

crystallites allowing the molecular chains of PVA to be more compact [93]. In addition,  $\text{CaCl}_2$  stabilizes the three dimensional network of SA molecules with minimal swelling ability [89].

Changes in area (Figure 22B) showed a slight increase of  $0.92 \pm 1.66\%$  for PVA/SA films (5wt%/1wt% blend) after 5 minutes of crosslinking, followed by a decrease of  $3.99 \pm 0.50\%$  and  $0.72 \pm 3.71\%$  after 10 and 30 minutes of crosslinking, respectively. The PVA/SA films (6wt%/1.2 wt% blend) showed decreases of  $4.34 \pm 1.07\%$  and  $0.72 \pm 0.74\%$  in area after 5 and 10 minutes of crosslinking, respectively. An increase in area of  $1.50 \pm 2.48\%$  was found after 30 minutes of crosslinking. The PVA-SA films (7wt%/1.4wt% blend) underwent a slight increase in area of  $0.87 \pm 3.97\%$  after 5 minutes of crosslinking time followed by decreases in area of  $3.53 \pm 3.83\%$  and  $0.72 \pm 4.27\%$  after 10 and 30 minutes of crosslinking, respectively. The data in area change showed no statistical significance between the samples and the crosslinking time. Studies suggested that SA had the potential to shrink/dissolve after crosslinking due to the presence of boric acid, whereas swelling could occur for PVA within the blend PVA/SA films [93,97].

The changes in thickness of PVA/SA films (5wt%/1wt% blend) showed no change after 5 and 30 minutes of crosslinking, whereas an increase of  $0.55 \pm 1.16\%$  in thickness was found after 10 minutes of crosslinking (Figure 22C). The changes in thickness were  $1.28 \pm 2.22\%$  and  $0.95 \pm 2.02\%$  for PVA/SA films (6wt%/1.2wt% blend) after 5 and 10 minutes of crosslinking, respectively. After 30 minutes of crosslinking time, the thickness of the film decreased  $0.72 \pm 1.54\%$ . The change in thickness of

PVA/SA films (7wt%/1.4wt% blend) underwent increases of  $1.45 \pm 2.51\%$  and  $1.01 \pm 1.75\%$  after 10 and 30 minutes of crosslinking, respectively. There was no thickness change on samples after 5 minutes of crosslinking. Minor changes in thickness were observed due to effects of hydrolytic degradation in SA and swelling of PVA from blend PVA/SA films [93,101] Overall, our methods showed the stabilization of PVA/SA chemical structure resulting in minimal morphological changes.

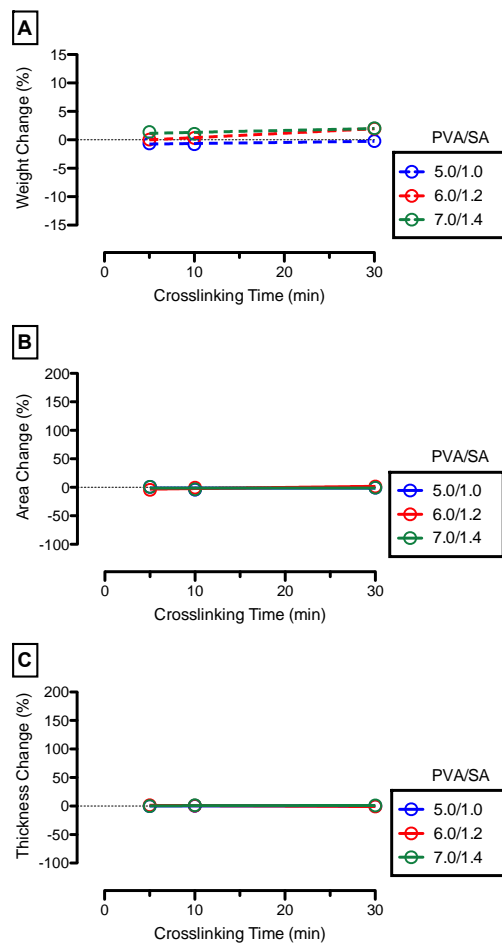


**Figure 25.** PVA/SA sample films crosslinked with the mixture of  $\text{CaCl}_2$ /boric acid solutions for 5, 10, and 30 minutes.

It is well known that the carboxylate groups of SA form hydrogen bonds with the hydroxyl group of PVA [102]. This effect explains the stabilization of PVA/SA films on their physical appearances during the crosslinking procedure. By nature, both PVA and SA are highly soluble in water and their solubility can be reduced by crosslinking where a stable 3D network of molecular structure is formed [103]. To achieve this properties, SA is crosslinked with  $\text{CaCl}_2$  which displace the  $\text{Na}^+$  ions with the  $\text{Ca}^{2+}$  ions that give more restrains to the SA molecule structure [104]. On the other hand, PVA is crosslinked with boric acid, resulting in limiting the mobility of the molecular chain due to hydrolysis [84]. In present study, both crosslinking techniques were utilized to enhance the stability of the molecular network of blend PVA/SA films. The resulting physical properties suggested that by controlling the thickness of the films through the adjustments of polymer concentrations during solvent casting, PVA/SA films had stable appearances suitable for practical uses in wound dressings.

#### *5.8 Chemical analyses: FTIR*

Fourier-transform infrared (FTIR) spectroscopy was used to analyze the changes in the molecular structure before and after crosslinking of the PVA/SA blend films at various thicknesses. Figure 23 showed the FTIR characteristics peaks of various thicknesses of PVA/SA samples, observed from  $700\text{ cm}^{-1}$  to  $4000\text{ cm}^{-1}$  wavenumbers, on the controls (uncrosslinked blend PVA/SA films) as well as the crosslinked PVA/SA films using a mixture of  $\text{CaCl}_2$  and boric acid for 5, 10, and 30 minutes, respectively. Table 7 listed the peak assignments for the characteristic peaks measured from PVA/SA films.

The FTIR spectra for the blends of PVA/SA films at various weight percent (i.e., thickness of the films) showed a characteristic broad band of intermolecular hydrogen bond (OH) between 3400 and 3200  $\text{cm}^{-1}$  related to the molecular structure of SA [78,95]. A characteristic band of alkyl ( $-\text{CH}_2$ ) stretching at between 2925 and 2853  $\text{cm}^{-1}$  and a characteristic band of C=O stretching, related to the primary amides and located between 1700 and 1600  $\text{cm}^{-1}$ , were observed in the spectra [78,95].

The FTIR spectra also revealed relevant data supported by literatures regarding the blend PVA/SA films. Specifically, the IR spectra showed a SA characteristic absorption band for carboxylic groups around 1419  $\text{cm}^{-1}$ , and an absorption peak was noted between 1150 – 1050  $\text{cm}^{-1}$  displaying the presence of the PVA structure [95]. Also, a weak band at around 1412  $\text{cm}^{-1}$  is related to ( $-\text{C-H}$ ) deformation in the ( $-\text{CH}_2$ ) groups [78]. A peak between 1,600  $\text{cm}^{-1}$  and 1,410  $\text{cm}^{-1}$  suggests a significant interaction between PVA and SA through alkyl ( $-\text{CH}_2$ ) groups, which is the formation of a hydrogen bond between the carboxyl group of SA and the hydroxyl group of PVA [95,102].

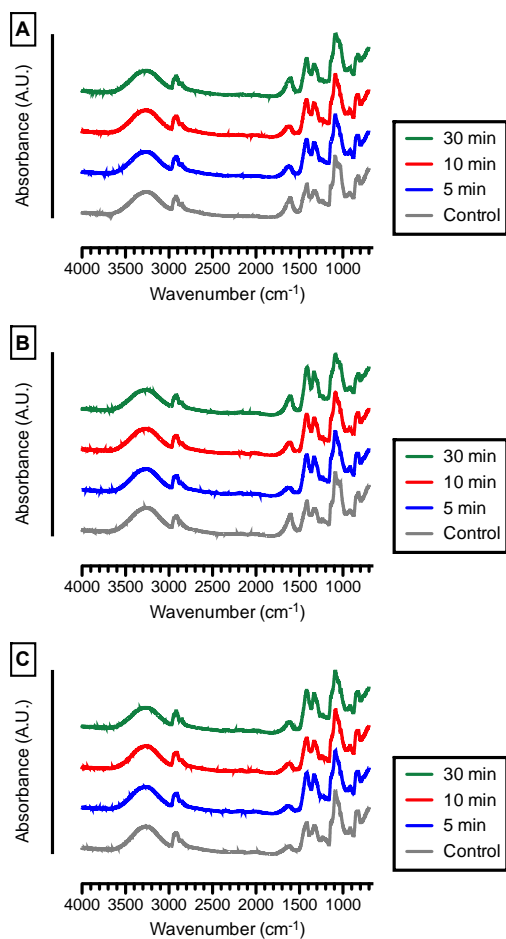


**Figure 26.** FTIR spectra of uncrosslinked blank PVA/SA films (Control) and crosslinked PVA/SA films with a mixture of  $\text{CaCl}_2$ /boric acid solutions for 5, 10, and 30 minutes, showing (a) 5wt%/1wt% PVA/SA, (b) 6wt%/1.2wt% PVA/SA, and (c) 7wt%/1.4wt% PVA/SA.

**Table 7.** Characteristics peaks observed on crosslinked PVA/SA films with CaCl<sub>2</sub> and boric acid for 5, 10, and 30 minutes and a PVA/SA blank film.

FTIR Analysis – Wavenumber (cm <sup>-1</sup> )				
Stretch	Control	PVA/SA (5wt%/1wt% blend) crosslinked with a		
	PVA/SA	mixture of CaCl <sub>2</sub> /boric acid solution		
	Films	5 min	10 min	30 min
C=O	1723	1729	1763	1769
C-H	2982	2995	2996	3000
O-H	3615	3625	3644	3645
Stretch	Control	PVA/SA (6wt%/1.2wt% blend) crosslinked with a		
	PVA/SA	mixture of CaCl <sub>2</sub> /boric acid solution		
	Films	5 min	10 min	30 min
C=O	1701	1740	1759	1765
C-H	2976	2983	2996	3007
O-H	3631	3645	3647	3676
Stretch	Control	PVA/SA (7wt%/1.4wt% blend) crosslinked with a		
	PVA/SA	mixture of CaCl <sub>2</sub> /boric acid solution		
	Films	5 min	10 min	30 min
C=O	1721	1746	1759	1765
C-H	3001	2996	2991	2990
O-H	3599	3610	3611	3647

### 5.9 PVA-SA Mechanical Properties

Uniaxial tensile tests were performed on crosslinked PVA/SA samples of various thicknesses. Five rectangular shape PVA/SA samples were used for tensile test to evaluate the changes in elastic modulus and the tensile strength due to crosslinking. The quantitative results of control (uncrosslinked) and crosslinked PVA/SA films on the elastic modulus and tensile strength are shown in Figure 24. The average values of elastic moduli and tensile strength are summarized in Table 8.

The average the average elastic moduli of PVA/SA films (5wt%/1wt% blend) crosslinked with a mixture of CaCl<sub>2</sub>/boric acid solutions for 5, 10, and 30 minutes were  $389 \pm 99$  MPa,  $399 \pm 42$  MPa, and  $518 \pm 55$  MPa, respectively. The elastic moduli of the 5- and 10-minute crosslinking samples were lower than that of the control groups ( $490 \pm 40$  MPa), sample without crosslinking. The average tensile strength of PVA/SA films (5wt%/1wt% blend) crosslinked with a mixture of CaCl<sub>2</sub>/boric acid solutions for 5, 10, and 30 minutes were  $28.1 \pm 2.4$  MPa,  $30.0 \pm 4.4$  MPa, and  $32.7 \pm 7.5$  MPa, respectively, whereas the uncrosslinked control groups received an average tensile strength of  $29.7 \pm 1.2$  MPa.

The average elastic moduli of PVA/SA films (6wt%/1.2wt% blend) crosslinked with a mixture of CaCl<sub>2</sub>/boric acid solutions for 5, 10, and 30 minutes were  $570 \pm 94$  MPa,  $601 \pm 93$  MPa, and  $963 \pm 83$  MPa, respectively. These values were considerably higher than that of the uncrosslinked control groups ( $538 \pm 133$  MPa). The average tensile strength of PVA/SA films (6wt%/1.2wt% blend) crosslinked with the a mixture of CaCl<sub>2</sub>/boric acid solutions for 5, 10, and 30 minutes were  $38.2 \pm 2.7$  MPa,  $35.0 \pm 1.0$

MPa, and  $52.7 \pm 14.6$  MPa, respectively, whereas the uncrosslinked control groups showed an average tensile strength of  $35.3 \pm 10.7$  MPa.

The average elastic moduli of PVA/SA films (7wt%/1.4wt% blend) crosslinked with a mixture of CaCl<sub>2</sub>/boric acid solutions for 5, 10, and 30 minutes were  $504 \pm 79$  MPa,  $716 \pm 50$  MPa, and  $1144 \pm 174$  MPa, respectively. These elastic moduli were significantly higher than that of the uncrosslinked control group ( $440 \pm 46$  MPa). The average tensile strength of PVA/SA films (7wt%/1.4wt% blend) crosslinked with a mixture of CaCl<sub>2</sub>/boric acid solutions for 5, 10, and 30 minutes were  $34.3 \pm 7.1$  MPa,  $35.3 \pm 8.4$  MPa, and  $42.0 \pm 1.0$  MPa, respectively, whereas the average tensile strength of the uncrosslinked control groups was  $28.7 \pm 2.3$  MPa.

Overall, the tendency on the average elastic modulus and the tensile strength after crosslinking of the blend PVA/SA films increased as increasing the crosslinking time. Moreover, our data suggested that increasing the weight percent of PVA/SA films (i.e., increase the thickness of the film), the mechanical properties of the corresponding membranes were enhanced.

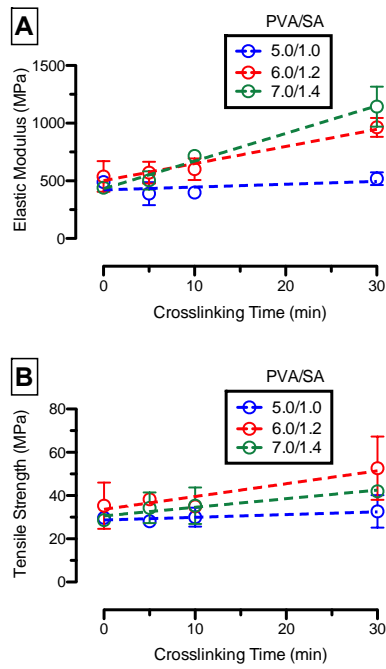


**Figure 27.** Mechanical properties of PVA/SA films showing (a) average elastic modulus and (b) average tensile strength after crosslinking in the mixture of  $\text{CaCl}_2$ /boric acid solutions for 5, 10, and 30 minutes.

**Table 8.** Mechanical properties of PVA/SA films crosslinked in the mixture of CaCl<sub>2</sub>/boric acid solution for 5, 10, and 30 min.

Mechanical Properties				
	Control	PVA/SA (5wt%/1wt% blend) crosslinked with a		
	PVA/SA	mixture of CaCl <sub>2</sub> /boric acid solution		
	Films	5 min	10 min	30 min
E (MPa)	490 ± 40	389 ± 99	399 ± 42	518 ± 55
σ <sub>T.S.</sub> (MPa)	29.7 ± 1.2	28.1 ± 2.4	30.0 ± 4.4	32.7 ± 7.5
	Control	PVA/SA (6wt%/1.2wt% blend) crosslinked with a		
	PVA/SA	mixture of CaCl <sub>2</sub> /boric acid solution		
	Films	5 min	10 min	30 min
E (MPa)	538 ± 133	570 ± 94	601 ± 93	963 ± 83
σ <sub>T.S.</sub> (MPa)	35.3 ± 10.7	38.2 ± 2.7	35.0 ± 1.0	52.7 ± 14.6
	Control	PVA/SA (7wt%/1.4wt% blend) crosslinked with a		
	PVA/SA	mixture of CaCl <sub>2</sub> /boric acid solution		
	Films	5 min	10 min	30 min
E (MPa)	440 ± 46	504 ± 79	716 ± 50	1144 ± 174
σ <sub>T.S.</sub> (MPa)	28.7 ± 2.3	34.3 ± 7.1	35.3 ± 8.4	42.0 ± 1.0

## Chapter 6: Conclusions and Future Work

In this research work, pure PVA, pure SA, and blend PVA/SA membranes were fabricated by solvent casting method followed by crosslinking methods in pure CaCl<sub>2</sub>, boric acid, and a mixture of CaCl<sub>2</sub>/Boric acid. The various films were studied considering their physical appearances, chemical compositions using FTIR, and mechanical properties using tensile testing to evaluate their potentials as a platform in wound dressing. Initial studies showed that pure PVA and pure SA films exhibited large deviations in physical and mechanical properties due to the distortion of their mechanical structure. Most importantly, the blend PVA/SA films maintained their physical shapes after crosslinking, suggesting an ideal processing parameter to proceed for film optimization.

According to all physical properties (e.g., weight, thickness, and area), thickness appears to be the dominating factor in influencing the mechanical properties of the crosslinked films. As a result, further exploration was carried out to study various concentrations of polymer solutions in solvent casting to achieve quality control on the final thickness of the cast films. Various weight fractions of PVA/SA membranes were produced and characterized for their physicochemical and mechanical properties targeting possible applications as a wound dressing. Results showed that crosslinking of PVA/SA films in a mixture of CaCl<sub>2</sub>/Boric acid solutions experienced minimal physical changes, suggesting an improvement in manufacturing and crosslinking processes.

After crosslinking, the chemical structure of the blend PVA/SA films showed a SA-related band of hydroxyl bond (O-H) stretching between 3400 and 3200 cm<sup>-1</sup>, a

carboxyl band (C=O) stretching between  $1700\text{ cm}^{-1}$  and  $1600\text{ cm}^{-1}$ , a C-H stretching between  $1700\text{ cm}^{-1}$  and  $1600\text{ cm}^{-1}$ , and a (-CH<sub>2</sub>) peak between  $1600\text{ cm}^{-1}$  and  $1410\text{ cm}^{-1}$  associated with interaction between carboxyl groups of SA and the hydroxyl groups of PVA. The study in chemical structure of the PVA/SA films by FTIR indicated the abilities in crosslinking of the polymers, which provides the potential platform in wound dressings.

The mechanical properties of the PVA/SA films showed that the average elastic moduli and average tensile strength increased with increasing crosslinking time in the mixture of CaCl<sub>2</sub>/boric acid solutions. The improvements in mechanical properties were supportive of the findings of chemical analysis work, suggesting a stronger molecular network after crosslinking. This study demonstrated that the physicochemical properties of the PVA/SA films were related to their corresponding mechanical properties, which is beneficial to the design and manufacturing of the film based wound dressing.

For future work, it is suggested to investigate the effects of various ratios of blend PVA/SA membrane, especially for those containing a higher amount of SA. Another area in the fabrication of PVA/SA membrane that is worthwhile to study is to explore the effects of various crosslinking times, less than 5 minutes, with different CaCl<sub>2</sub> and boric acid content in the crosslinking solution. The content of the polymer, the concentration of the crosslinking solutions, and the crosslinking time may have significant implication in the dissolution properties of the membranes. Other suggested characterization methods include water contact angle study and differential scanning calorimetry (DSC) to understand the surface and thermal properties of the membrane, respectively. Finally, it is

suggested that with the membranes can be loaded with various small molecule drugs for the investigations on the effects of crosslinking of PVA/SA membranes for drug delivery.

## References

- [1] S.C. Wu, D.G. Armstrong, Clinical outcome of diabetic foot ulcers treated with negative pressure wound therapy and the transition from acute care to home care, *International Wound Journal*. 5 (2008) 10–16.
- [2] S.P. Pendsey, Understanding diabetic foot, *International Journal of Diabetes in Developing Countries*. 30 (2010) 75–79.
- [3] C.K. Sen, G.M. Gordillo, S. Roy, R. Kirsner, L. Lambert, T.K. Hunt, et al., Human skin wounds: A major and snowballing threat to public health and the economy, *Wound Repair and Regeneration*. 17 (2009) 763–771.
- [4] Centers for Disease Control and Prevention, Hospital Discharge Rates for Ulcer/Inflammation/Infection (ULCER) as First-Listed Diagnosis per 1,000 Diabetic Population, by Age, United States, 1988–2007, Atlanta, GA, 2014.  
[https://www.cdc.gov/diabetes/statistics/hosplea/diabetes\\_complications/fig3\\_ulcer.htm](https://www.cdc.gov/diabetes/statistics/hosplea/diabetes_complications/fig3_ulcer.htm) (accessed September 9, 2019).
- [5] C.W. Hicks, S. Selvarajah, N. Mathioudakis, R.L. Sherman, K.F. Hines, J.H. Black, et al., Burden of infected diabetic foot ulcers on hospital admissions and costs, *Annals of Vascular Surgery*. 33 (2016) 149–158.
- [6] R.S. Ambekar, B. Kandasubramanian, Advancements in nanofibers for wound dressing: A review, *European Polymer Journal*. 117 (2019) 304–336.
- [7] J.S. Boateng, K.H. Matthews, H.N.E. Stevens, G.M. Eccleston, Wound healing dressings and drug delivery systems: A review, *Journal of Pharmaceutical Sciences*. 97 (2008) 2892–2923.

- [8] E.A. Kamoun, E.-R.S. Kenawy, T.M. Tamer, M.A. El-Meligy, M.S. Mohy Eldin, Poly(vinyl alcohol)-alginate physically crosslinked hydrogel membranes for wound dressing applications: Characterization and bio-evaluation, *Arabian Journal of Chemistry*. 8 (2015) 38–47.
- [9] S. Tyeb, N. Kumar, A. Kumar, V. Verma, Flexible agar-sericin hydrogel film dressing for chronic wounds, *Carbohydrate Polymers*. 200 (2018) 572–582.
- [10] O.L. Shanmugasundaram, K. Syed Zameer Ahmed, K. Sujatha, P. Ponnmurugan, A. Srivastava, R. Ramesh, et al., Fabrication and characterization of chicken feather keratin/polysaccharides blended polymer coated nonwoven dressing materials for wound healing applications, *Materials Science and Engineering: C*. 92 (2018) 26–33.
- [11] S.P. Miguel, D.R. Figueira, D. Simões, M.P. Ribeiro, P. Coutinho, P. Ferreira, et al., Electrospun polymeric nanofibres as wound dressings: A review, *colloids and surfaces B: Biointerfaces*. 169 (2018) 60–71.
- [12] S. Patel, S. Srivastava, M.R. Singh, D. Singh, Mechanistic insight into diabetic wounds: Pathogenesis, molecular targets and treatment strategies to pace wound healing, *Biomedicine & Pharmacotherapy*. 112 (2019) 108615.
- [13] T. Velnar, T. Bailey, V. Smrkolj, The Wound Healing Process: An overview of the cellular and molecular mechanisms, *Journal of International Medical Research*. 37 (2009) 1528–1542.

- [14] G. Castellanos, Á. Bernabé-García, J.M. Moraleda, F.J. Nicolás, Amniotic membrane application for the healing of chronic wounds and ulcers, *Placenta*. 59 (2017) 146–153.
- [15] P.-H. Wang, B.-S. Huang, H.-C. Horng, C.-C. Yeh, Y.-J. Chen, Wound healing, *Journal of the Chinese Medical Association*. 81 (2018) 94–101.
- [16] D. Harper, A. Young, C.-E. McNaught, The physiology of wound healing, *Surgery (Oxford)*. 32 (2014) 445–450.
- [17] J.M. Reinke, H. Sorg, Wound repair and regeneration, *European Surgical Research*. 49 (2012) 35–43.
- [18] G. Hosgood, Stages of wound healing and their clinical relevance, *Veterinary Clinics of North America: Small Animal Practice*. 36 (2006) 667–685.
- [19] N.X. Landén, D. Li, M. Ståhle, Transition from inflammation to proliferation: a critical step during wound healing, *cellular and molecular life sciences*. 73 (2016) 3861–3885.
- [20] S. Singh, A. Young, C.-E. McNaught, The physiology of wound healing, *Surgery (Oxford)*. 35 (2017) 473–477.
- [21] T. Wilgus, Immune cells in the healing skin wound: Influential players at each stage of repair, *Pharmacological Research*. 58 (2008) 112–116.
- [22] H. Eo, H.-J. Lee, Y. Lim, Ameliorative effect of dietary genistein on diabetes induced hyper-inflammation and oxidative stress during early stage of wound healing in alloxan induced diabetic mice, *Biochemical and Biophysical Research Communications*. 478 (2016) 1021–1027.

- [23] L.-J. Li, X.-H. Xu, T.-J. Yuan, J. Hou, C.-L. Yu, L.-H. Peng, *Periplaneta Americana* L. as a novel therapeutics accelerates wound repair and regeneration, *Biomedicine & Pharmacotherapy*. 114 (2019) 108858.
- [24] L. Su, J. Zheng, Y. Wang, W. Zhang, D. Hu, Emerging progress on the mechanism and technology in wound repair, *Biomedicine & Pharmacotherapy*. 117 (2019) 109191.
- [25] M. Takeo, W. Lee, M. Ito, Wound healing and skin regeneration, *Cold Spring Harbor Perspectives in Medicine*. 5 (2015) a023267–a023267.
- [26] S.A. Shah, M. Sohail, S. Khan, M.U. Minhas, M. de Matas, V. Sikstone, et al., Biopolymer-based biomaterials for accelerated diabetic wound healing: a critical review, *International Journal of Biological Macromolecules*. 139 (2019) 975–993.
- [27] A. Abou-Okeil, H.M. Fahmy, M.K. El-Bisi, O.A. Ahmed-Farid, Hyaluronic acid/Na-alginate films as topical bioactive wound dressings, *European Polymer Journal*. 109 (2018) 101–109.
- [28] E.S. Gil, B. Panilaitis, E. Bellas, D.L. Kaplan, Functionalized silk biomaterials for wound healing, *Advanced Healthcare Materials*. 2 (2013) 206–217.
- [29] J.W. Penn, A.O. Grobbelaar, K.J. Rolfe, The role of the TGF- $\beta$  family in wound healing, burns and scarring: a review, *International Journal of Burns and Trauma*. 2 (2012) 18–28.
- [30] R.F. Diegelmann, Wound healing: an overview of acute, fibrotic and delayed healing, *Frontiers in Bioscience*. 9 (2004) 283.

- [31] M.M.G. Fouda, R. Wittke, D. Knittel, E. Schollmeyer, Use of chitosan/polyamine biopolymers based cotton as a model system to prepare antimicrobial wound dressing, *International Journal of Diabetes Mellitus*. 1 (2009) 61–64.
- [32] S.-Y. Lin, K.-S. Chen, L. Run-Chu, Design and evaluation of drug-loaded wound dressing having thermoresponsive, adhesive, absorptive and easy peeling properties, *Biomaterials*. 22 (2001) 2999–3004.
- [33] H.S. Kim, X. Sun, J.-H. Lee, H.-W. Kim, X. Fu, K.W. Leong, Advanced drug delivery systems and artificial skin grafts for skin wound healing, *Advanced Drug Delivery Reviews*. 146 (2019) 209–239.
- [34] M.C. García, A.A. Aldana, L.I. Tártara, F. Alovero, M.C. Strumia, R.H. Manzo, et al., Bioadhesive and biocompatible films as wound dressing materials based on a novel dendronized chitosan loaded with ciprofloxacin, *Carbohydrate Polymers*. 175 (2017) 75–86.
- [35] Q. Chen, J. Wu, Y. Liu, Y. Li, C. Zhang, W. Qi, et al., Electrospun chitosan/PVA/bioglass Nanofibrous membrane with spatially designed structure for accelerating chronic wound healing, *Materials Science and Engineering: C*. 105 (2019) 110083.
- [36] S. Vakilian, F. Jamshidi-adevani, S. Al-Shidhani, M.U. Anwar, R. Al-Harrasi, N. Al-Wahaibi, et al., A Keratin-based biomaterial as a promising dresser for skin wound healing, *Wound Medicine*. 25 (2019) 100155.
- [37] G.T. Voss, M.S. Gularte, A.G. Vogt, J.L. Giongo, R.A. Vaucher, J.V.Z. Echenique, et al., Polysaccharide-based film loaded with vitamin C and propolis: A promising

device to accelerate diabetic wound healing, *International Journal of Pharmaceutics*. 552 (2018) 340–351.

- [38] A. Sionkowska, Current research on the blends of natural and synthetic polymers as new biomaterials: review, *Progress in Polymer Science*. 36 (2011) 1254–1276.
- [39] G. Heness, B. Ben-Nissan, Innovative bioceramics, *Materials Forum*. 27 (2004) 104–144.
- [40] S.A. Shah, M. Sohail, S. Khan, M.U. Minhas, M. de Matas, V. Sikstone, et al., Biopolymer-based biomaterials for accelerated diabetic wound healing: a critical review, *International Journal of Biological Macromolecules*. 139 (2019) 975–993.
- [41] M.J. Byrom, P.G. Bannon, G.H. White, M.K.C. Ng, Animal models for the assessment of novel vascular conduits, *Journal of Vascular Surgery*. 52 (2010) 176–195.
- [42] M. Small, A. Faglie, A. Craig, M. Pieper, V. Fernand Narcisse, P. Neuenschwander, et al., Nanostructure-enabled and macromolecule-grafted surfaces for biomedical applications, *Micromachines*. 9 (2018) 243.
- [43] A.D. Metcalfe, M.W.J. Ferguson, Tissue engineering of replacement skin: the crossroads of biomaterials, wound healing, embryonic development, stem cells and regeneration, *Journal of The Royal Society Interface*. 4 (2007) 413–437.
- [44] C. Alemdaroğlu, Z. Değim, N. Çelebi, F. Zor, S. Öztürk, D. Erdoğan, An investigation on burn wound healing in rats with chitosan gel formulation containing epidermal growth factor, *Burns*. 32 (2006) 319–327.

- [45] M. Li, M. Han, Y. Sun, Y. Hua, G. Chen, L. Zhang, Oligoarginine mediated collagen/chitosan gel composite for cutaneous wound healing, *International Journal of Biological Macromolecules*. 122 (2019) 1120–1127.
- [46] M. Jridi, S. Sellimi, K.B. Lassoued, S. Beltaief, N. Souissi, L. Mora, et al., Wound healing activity of cuttlefish gelatin gels and films enriched by henna (*Lawsonia inermis*) extract, *Colloids and Surfaces A: Physicochemical and Engineering Aspects*. 512 (2017) 71–79.
- [47] C.C. Yates, D. Whaley, R. Babu, J. Zhang, E. Beckman, A.W. Pasculle, et al., The effect of multifunctional polymer-based gels on wound healing in full thickness bacteria-contaminated mouse models, *Biomaterials*. 28 (2007) 3977–3986.
- [48] P.K. Sehgal, R. Sripriya, M. Senthilkumar, S. Rajendran, Drug delivery dressings, in: *Advanced Textiles for Wound Care*, Elsevier, 2019: pp. 261–288.
- [49] F.-L. Mi, Y.-B. Wu, S.-S. Shyu, A.-C. Chao, J.-Y. Lai, C.-C. Su, Asymmetric chitosan membranes prepared by dry/wet phase separation: a new type of wound dressing for controlled antibacterial release, *Journal of Membrane Science*. 212 (2003) 237–254.
- [50] J.S. Boateng, K.H. Matthews, H.N.E. Stevens, G.M. Eccleston, Wound healing dressings and drug delivery systems: a review, *Journal of Pharmaceutical Sciences*. 97 (2008) 2892–2923.
- [51] H. Zhou, C. Liang, Z. Wei, Y. Bai, S.B. Bhaduri, T.J. Webster, et al., Injectable biomaterials for translational medicine, *Materials Today*. 28 (2019) 81–97.

- [52] H. Uludağ, Grand challenges in biomaterials, *Frontiers in Bioengineering and Biotechnology*. 2 (2014) 43.
- [53] E.A. Kamoun, X. Chen, M.S. Mohy Eldin, E.-R.S. Kenawy, Crosslinked poly(vinyl alcohol) hydrogels for wound dressing applications: A review of remarkably blended polymers, *Arabian Journal of Chemistry*. 8 (2015) 1–14.
- [54] K. Shanmugapriya, H. Kim, P.S. Saravana, B.-S. Chun, H.W. Kang, Fabrication of multifunctional chitosan-based nanocomposite film with rapid healing and antibacterial effect for wound management, *International Journal of Biological Macromolecules*. 118 (2018) 1713–1725.
- [55] G.T. Voss, M.S. Gularte, A.G. Vogt, J.L. Giongo, R.A. Vaucher, J.V.Z. Echenique, et al., Polysaccharide-based film loaded with vitamin C and propolis: A promising device to accelerate diabetic wound healing, *International Journal of Pharmaceutics*. 552 (2018) 340–351.
- [56] N. Üstündağ Okur, N. Hökenek, M.E. Okur, Ş. Ayla, A. Yoltaş, P.I. Sifaka, et al., An alternative approach to wound healing field; new composite films from natural polymers for mupirocin dermal delivery, *Saudi Pharmaceutical Journal*. 27 (2019) 738–752.
- [57] N. Kanasan, S. Adzila, N. AzimahMustaffa, P. Gurubaran, The effect of sodium alginate on the properties of hydroxyapatite, *Procedia Engineering*. 184 (2017) 442–448.

- [58] M. Bruchet, A. Melman, Fabrication of patterned calcium cross-linked alginate hydrogel films and coatings through reductive cation exchange, *Carbohydrate Polymers*. 131 (2015) 57–64.
- [59] S.R. Moxon, N.J. Corbett, K. Fisher, G. Potjewyd, M. Domingos, N.M. Hooper, Blended alginate/collagen hydrogels promote neurogenesis and neuronal maturation, *Materials Science and Engineering: C*. 104 (2019) 109904.
- [60] A. Can Karaca, I.G. Erdem, M.M. Ak, Effects of polyols on gelation kinetics, gel hardness, and drying properties of alginates subjected to internal gelation, *LWT*. 92 (2018) 297–303.
- [61] H. Zhou, S. Kong, Z. Liu, Y. Pan, Y. Liu, M. Luo, et al., Fabrication and evaluation of calcium alginate/ calcium polyphosphate composite, *Materials Letters*. 180 (2016) 184–187.
- [62] S. Karki, H. Kim, S.-J. Na, D. Shin, K. Jo, J. Lee, Thin films as an emerging platform for drug delivery, *Asian Journal of Pharmaceutical Sciences*. 11 (2016) 559–574.
- [63] G.T. Grant, E.R. Mon, S.D.A. Rees, Biological interactions between polysaccharides and divalent cations: the egg-box model, *FEBS Letters*. 32 (1973) 195–198.
- [64] M. Baniyadi, M. Minary-Jolandan, Alginate-collagen fibril composite hydrogel, *Materials*. 8 (2015) 799–814.
- [65] S.F. Wee, W.R. Gombotz, Protein release from alginate matrices, *Advanced Drug Delivery Reviews*. 31 (1998) 267–285.

- [66] K.Y. Lee, D.J. Mooney, Alginate: properties and biomedical applications, *Progress in Polymer Science*. 37 (2012) 106–126.
- [67] P. Vanstraelen, Comparison of calcium sodium alginate (KALTOSTAT) and porcine xenograft (E-Z DERM) in the healing of split-thickness skin graft donor sites, *Burns*. 18 (1992) 145–148.
- [68] R.G. Pillai, Z. Al Naieb, Plastibell circumcision supported by a calcium-alginate fibre dressing to reduce bleeding, *Arab Journal of Urology*. 13 (2015) 179–181.
- [69] R.B. Davey, A.L. Sparnon, R.W. Byard, Unusual donor site reactions to calcium alginate dressings, *Burns*. 26 (2000) 393–398.
- [70] T. Wang, Q. Gu, J. Zhao, J. Mei, M. Shao, Y. Pan, et al., Calcium alginate enhances wound healing by up-regulating the ratio of collagen types I/III in diabetic rats, *International Journal of Clinical and Experimental Pathology*. 8 (2016) 6636–6645.
- [71] S. Karki, H. Kim, S.J. Na, D. Shin, K. Jo, J. Lee, Thin films as an emerging platform for drug delivery, *Asian Journal of Pharmaceutical Sciences*. 11 (2016) 559–574.
- [72] J. Renukuntla, A.D. Vadlapudi, A. Patel, S.H. Boddu, A.K. Mitra, Approaches for enhancing oral bioavailability of peptides and proteins, *International Journal of Pharmaceutics*. 447 (2013) 75–93.
- [73] M.E. Dmitrenko, A.V. Penkova, A.I. Kuzminova, M. Morshed, M.I. Larionov, H. Alem, et al., Investigation of new modification strategies for PVA membranes to improve their dehydration properties by pervaporation, *Applied Surface Science*. 450 (2018) 527–537.

- [74] T. Gaaz, A. Sulong, M. Akhtar, A. Kadhum, A. Mohamad, A. Al-Amiery, Properties and applications of polyvinyl alcohol, halloysite nanotubes and their nanocomposites, *Molecules*. 20 (2015) 22833–22847.
- [75] M. Wang, J. Li, W. Li, Z. Du, S. Qin, Preparation and characterization of novel poly(vinyl alcohol)/collagen double-network hydrogels, *International Journal of Biological Macromolecules*. 118 (2018) 41–48.
- [76] J.-S. Park, J.-W. Park, E. Ruckenstein, Thermal and dynamic mechanical analysis of PVA/MC blend hydrogels, *Polymer*. 42 (2001) 4271–4280.
- [77] S. Jiang, S. Liu, W. Feng, PVA hydrogel properties for biomedical application, *Journal of the Mechanical Behavior of Biomedical Materials*. 4 (2011) 1228–1233.
- [78] J.A.P. Dutra, S.G. Carvalho, A.C.D. Zampiroli, R.D. Daltoé, R.M. Teixeira, F.P. Careta, et al., Papain wound dressings obtained from poly(vinyl alcohol)/calcium alginate blends as new pharmaceutical dosage form: preparation and preliminary evaluation, *European Journal of Pharmaceutics and Biopharmaceutics*. 113 (2017) 11–23.
- [79] I. Bano, M. Arshad, T. Yasin, M.A. Ghauri, M. Younus, Chitosan: a potential biopolymer for wound management, *International Journal of Biological Macromolecules*. 102 (2017) 380–383.
- [80] H. He, R. Cai, Y. Wang, G. Tao, P. Guo, H. Zuo, et al., Preparation and characterization of silk sericin/PVA blend film with silver nanoparticles for potential antimicrobial application, *International Journal of Biological Macromolecules*. 104 (2017) 457–464.

- [81] M.V. Cruz, A.C. Jacobowski, M.L.R. Macedo, K.A. Batista, K.F. Fernandes, Immobilization of antimicrobial trypsin inhibitors onto cashew gum polysaccharide/PVA films, *International Journal of Biological Macromolecules*. 127 (2019) 433–439.
- [82] M. Abbas, T. Hussain, M. Arshad, A.R. Ansari, A. Irshad, J. Nisar, et al., Wound healing potential of curcumin cross-linked chitosan/polyvinyl alcohol, *International Journal of Biological Macromolecules*. 140 (2019) 871–876.
- [83] J.M. Gohil, A. Bhattacharya, P. Ray, Studies on the crosslinking of poly(vinyl alcohol), *Journal of Polymer Research*. 13 (2006) 161–169.
- [84] K. Ye, Y. Li, W. Zhang, Q. Zhang, W. Chen, L. Meng, et al., Stretch-induced structural evolution of poly(vinyl alcohol) at different concentrations of boric acid: An in-situ synchrotron radiation small- and wide- angle x-ray scattering study, *Polymer Testing*. 77 (2019) 105913.
- [85] B. Bolto, T. Tran, M. Hoang, Z. Xie, Crosslinked poly(vinyl alcohol) membranes, *Progress in Polymer Science*. 34 (2009) 969–981.
- [86] C.M. Hassan, N.A. Peppas, Structure and morphology of freeze/thawed PVA hydrogels, *Macromolecules*. 33 (2000) 2472–2479.
- [87] M. Ferry, Y. Ngono-Ravache, C. Aymes-Chodur, M.C. Clochard, X. Coqueret, L. Cortella, et al., Ionizing radiation effects in polymers, in: *Reference Module in Materials Science and Materials Engineering*, Elsevier, 2016.
- [88] M.M.S. Lencina, N.A. Andreucetti, C.G. Gómez, M.A. Villar, Recent studies on alginates based blends, composites, and nanocomposites, in: S. Thomas, P.M.

Visakh, Aji.P. Mathew (Eds.), *Advances in Natural Polymers*, Springer Berlin Heidelberg, Berlin, Heidelberg, 2013: pp. 193–254.

- [89] A. Saarai, V. Kasparkova, T. Sedlacek, P. Saha, A comparative study of crosslinked sodium alginate/gelatin hydrogels for wound dressing, in *Proceedings of the 4th WSEAS international conference on Energy and development - environment – biomedicine*. (2011) 384–389
- [90] N.E. Simpson, C.L. Stabler, C.P. Simpson, A. Sambanis, I. Constantinidis, The role of the CaCl<sub>2</sub>–guluronic acid interaction on alginate encapsulated  $\beta$ TC3 cells, *Biomaterials*. 25 (2004) 2603–2610.
- [91] S.-F. Chou, K.A. Woodrow, Relationships between mechanical properties and drug release from electrospun fibers of PCL and PLGA blends, *Journal of the Mechanical Behavior of Biomedical Materials*. 65 (2017) 724–733.
- [92] J.S. Boateng, K.H. Matthews, H.N.E. Stevens, G.M. Eccleston, Wound healing dressings and drug delivery systems: a review, *Journal of Pharmaceutical Sciences*. 97 (2008) 2892–2923.
- [93] M. Lim, H. Kwon, D. Kim, J. Seo, H. Han, S.B. Khan, Highly-enhanced water resistant and oxygen barrier properties of cross-linked poly(vinyl alcohol) hybrid films for packaging applications, *Progress in Organic Coatings*. 85 (2015) 68–75.
- [94] J.N. BeMiller, *Algins/alginate*, in: *Carbohydrate Chemistry for Food Scientists*, Elsevier, 2019: pp. 293–301.

- [95] E.A. Kamoun, X. Chen, M.S. Mohy Eldin, E.-R.S. Kenawy, Crosslinked poly(vinyl alcohol) hydrogels for wound dressing applications: A review of remarkably blended polymers, *Arabian Journal of Chemistry*. 8 (2015) 1–14.
- [96] L.A. Loureiro dos Santos, *Natural Polymeric Biomaterials: Processing and Properties*, in: *Reference Module in Materials Science and Materials Engineering*, Elsevier, 2017.
- [97] S.M.M. Quintero, R.V. Ponce F, M. Cremona, A.L.C. Triques, A.R. d’Almeida, A.M.B. Braga, Swelling and morphological properties of poly(vinyl alcohol) (PVA) and poly(acrylic acid) (PAA) hydrogels in solution with high salt concentration, *Polymer*. 51 (2010) 953–958.
- [98] E.A. Kamoun, E.-R.S. Kenawy, T.M. Tamer, M.A. El-Meligy, M.S. Mohy Eldin, Poly (vinyl alcohol)-alginate physically crosslinked hydrogel membranes for wound dressing applications: characterization and bio-evaluation, *Arabian Journal of Chemistry*. 8 (2015) 38–47.
- [99] S. Udaseen, S. Asthana, N.T. Raveendran, K. Kumar, A. Samal, K. Pal, et al., Optimization of process parameters for nozzle - free electrospinning of poly(vinyl alcohol) and alginate blend nano-fibrous scaffolds, *International Journal of Enhanced Research in Science Technology & Engineering*. 3 (2014) 405–411.
- [100] J.M. Seok, S.H. Oh, S.J. Lee, J.H. Lee, W.D. Kim, S.-H. Park, et al., Fabrication and characterization of 3D scaffolds made from blends of sodium alginate and poly(vinyl alcohol), *Materials Today Communications*. (2018).

- [101] E.A. Kamoun, X. Chen, M.S. Mohy Eldin, E.-R.S. Kenawy, Crosslinked poly(vinyl alcohol) hydrogels for wound dressing applications: a review of remarkably blended polymers, *Arabian Journal of Chemistry*. 8 (2015) 1–14.
- [102] X. Sun, H. Uyama, A poly(vinyl alcohol)/sodium alginate blend monolith with nanoscale porous structure, *Nanoscale Research Letters*. 8 (2013) 411.
- [103] E.A. Kamoun, E.-R.S. Kenawy, T.M. Tamer, M.A. El-Meligy, M.S. Mohy Eldin, Poly(vinyl alcohol)-alginate physically crosslinked hydrogel membranes for wound dressing applications: characterization and bio-evaluation, *Arabian Journal of Chemistry*. 8 (2015) 38–47.
- [104] K.T. Shalumon, K.H. Anulekha, S.V. Nair, S.V. Nair, K.P. Chennazhi, R. Jayakumar, Sodium alginate/poly(vinyl alcohol)/nano ZnO composite nanofibers for antibacterial wound dressings, *International Journal of Biological Macromolecules*. 49 (2011) 247–254.